27717

National Library of Canada / Bibliothèque nationale du Canada

CANADIAN THESES ON MICROFICHE / THÈSES CANADIENNES SUR MICROFICHE

NAME OF AUTHOR/*NOM DE L'AUTEUR* ASGHAR IBN NOOR

TITLE OF THESIS/*TITRE DE LA THÈSE* The high pressure Langmuir probe in a weak flowing plasma and a plasma sheath

UNIVERSITY/*UNIVERSITÉ* The University of Alberta

DEGREE FOR WHICH THESIS WAS PRESENTED/ *GRADE POUR LEQUEL CETTE THÈSE FUT PRÉSENTÉE* M.Sc.

YEAR THIS DEGREE CONFERRED/*ANNÉE D'OBTENTION DE CE GRADE*

NAME OF SUPERVISOR/*NOM DU DIRECTEUR DE THÈSE* Dr. P.R. Smy

Permission is hereby granted to the NATIONAL LIBRARY OF CANADA to microfilm this thesis and to lend or sell copies of the film.

The author reserves other publication rights, and neither the thesis nor extensive extracts from it may be printed or otherwise reproduced without the author's written permission.

L'autorisation est, par la présente, accordée à la BIBLIOTHÈQUE NATIONALE DU CANADA de microfilmer cette thèse et de prêter ou de vendre des exemplaires du film.

L'auteur se réserve les autres droits de publication; ni la thèse ni de longs extraits de celle-ci ne doivent être imprimés ou autrement reproduits sans l'autorisation écrite de l'auteur.

DATED/*DATÉ* Dec 12/75 SIGNED/*SIGNÉ* A.I. Noor

PERMANENT ADDRESS/*RÉSIDENCE FIXÉ* c/o NOOR Muhammad
Sharagachi, Godagari, ~~Bangladesh~~
Rajshahi, Bangladesh.

NL-91 (3-74)

INFORMATION TO USERS

THIS DISSERTATION HAS BEEN
MICROFILMED EXACTLY AS RECEIVED

This copy was produced from a microfiche copy of the original document. The quality of the copy is heavily dependent upon the quality of the original thesis submitted for microfilming. Every effort has been made to ensure the highest quality of reproduction possible.

PLEASE NOTE: Some pages may have indistinct print. Filmed as received.

Canadian Theses Division
Cataloguing Branch
National Library of Canada
Ottawa, Canada K1A ON4

AVIS AUX USAGERS

LA THESE A ETE MICROFILMEE
TELLE QUE NOUS L'AVONS REÇUE

Cette copie a été faite à partir d'une microfiche du document original. La qualité de la copie dépend grandement de la qualité de la thèse soumise pour le microfimage. Nous avons tout fait pour assurer une qualité supérieure de reproduction.

NOTA BENE: La qualité d'impression de certaines pages peut laisser à désirer. Microfilmée telle que nous l'avons reçue.

Division des thèses canadiennes
Direction du catalogage
Bibliothèque nationale du Canada
Ottawa, Canada K1A ON4

THE UNIVERSITY OF ALBERTA

THE HIGH PRESSURE LANGMUIR PROBE IN A WEAK FLOWING PLASMA AND A PLASMA SHEATH

by

ASGHAR IBN NOOR (C)

A THESIS

SUBMITTED TO THE FACULTY OF GRADUATE STUDIES AND RESEARCH IN PARTIAL FULFILMENT OF THE REQUIREMENT FOR THE DEGREE OF

MASTER OF SCIENCE

DEPARTMENT OF ELECTRICAL ENGINEERING

EDMONTON, ALBERTA

SPRING 1976

THE UNIVERSITY OF ALBERTA

RELEASE FORM

NAME OF AUTHOR Asghar Ibn Noor

TITLE OF THESIS The High Pressure Langmuir Probe in a Weak Flowing Plasma and a Plasma Sheath

DEGREE FOR WHICH THESIS WAS PRESENTED Master of Science

YEAR THIS DEGREE GRANTED Spring 1976

Permission is hereby granted to THE UNIVERSITY OF ALBERTA LIBRARY to reproduce single copies of this thesis and to lend or sell such copies for private, scholarly or scientific research purposes only.

The author reserves other publication rights, and neither the thesis nor extensive extracts from it may be printed or otherwise reproduced without the author's written permission.

Signed A. I. Noor

Permanent Address

Sharagachi, Godagoni

Rajshahi

Bangladesh

Dated Dec 12 —, 1975

THE UNIVERSITY OF ALBERTA

FACULTY OF GRADUATE STUDIES AND RESEARCH

The undersigned certify that they have read, and recommend to the Faculty of Graduate Studies and Research, for acceptance, a thesis entitled THE HIGH PRESSURE LANGMUIR PROBE IN A WEAK FLOWING PLASMA AND A PLASMA SHEATH submitted by Asghar Ibn NOOR in partial fulfilment of the requirements for the degree of Master of Science.

Peter R Smy
.....
Supervisor

.....

.....

.....

.....

Date: Oct - 8 - 1975

ABSTRACT

An experimental investigation has been carried out to demonstrate that the well known sheath/convection and sheath/diffusion theories are not applicable to measurements of the electron density of dilute high pressure flowing plasmas using an ion probe.

It has been found that at low ionization densities, the current is no longer space charge limited but is in fact limited by the electric field generated by the probe. Experimental measurements with a cylindrical probe at densities down to $10^{12}/m^3$ show good agreement with the concept of a field limited current.

ACKNOWLEDGEMENTS

I wish to thank Dr. P.R. Smy for his patient supervision and encouragement during the course of this research.

I am indebted to all members of the plasma group for many helpful suggestions. I am thankful to Mr. P. Haswell for help in setting up the experiments.

Finally, I am grateful to the Department of Electrical Engineering and the National Research Council of Canada for financial assistance which made this thesis possible.

LIST OF SYMBOLS

R_e = Electric Reynolds number

v_f = Plasma convection velocity

r_p = Probe radius

D_i = Positive ion diffusivity

$$\alpha = \frac{\text{Debye Length}}{\text{Probe Radius}} = \frac{\sqrt{\frac{\varepsilon_o kT_e}{n_e e^2}}}{r_p}$$

ε_o = Permittivity of free space

k = Boltzmann's constant

T_e = Electron temperature.

n_e = Electron density

e = Electronic charge

$$x = \frac{eV}{kT_e}$$

V = Probe potential (Negative)

μ_i = Ionic mobility

E = Electric field

n_o = Ion density

Q = Charge per unit length on the probe

v = Velocity of ions relative to the probe

$$X = \frac{2\pi\varepsilon_o v_f x}{Q\mu_i}$$

$$Y = \frac{2\pi\varepsilon_o v_f y}{Q\mu_i}$$

I_p = Probe current per unit length

ϕ = The angle between the velocity and positive vectors.

CONTENTS

CHAPTER			Page
I	-	Introduction	1
	1.1	Flame as a plasma source	1
	1.2	Electrostatic probe as a plasma diagnostic	3
	1.3	Electrostatic probe for the diagnostics of flowing plasmas	5
	1.4	The nature of the present work	9
11	-	Theory	12
	2.1	The limit of space charge and field limited current	12
	2.2	Thin probe cylindrical geometry	18
	2.3	Thick probe cylindrical geometry	27
	2.4	Spherical probe geometry	30
	2.5	Probe measurement in an externally generated thick sheath	31
111	-	Experiment	35
	3.1	The burner system	35
	3.2	Flame ionization	39
	3.3	Ionization in the presence of additives	42
	3.4	Structure of the Langmuir probe	46

CONTENTS

CHAPTER		Page
3.5	Structure of the grid	46
3.6	Electron density measurement	48
3.7	Measurement of ion-density in a planar sheath	49
3.8	The velocity and temperature measurement at the top of chimney	51
IV -	Discussion	55
V -	Conclusion	64
-	References	67

LIST OF FIGURES

FIGURE		PAGE
1(a)	Sheath/convection model from ref.-21. All ions convected into the sheath eventually arrive at the probe.	16
1(b)	Field limited model. Only the ions in the band AA reach the probe.	16
1(c)	Planar sheath model. E_o is the local field.	16
1(d)	Coordinate system for equations (13) and equation (14).	20
1(e)	The trajectories of the particles very close to a probe, due to inviscid flow.	28
2	Trajectories for ions having different impact parameters solved from eqn. (15)	23
3	The experimental setup of the burner.	38
4	Flame without chimney and with a chimney at the top.	40
5	Flame with a chimney at the bottom.	41
6	Fall-off of ionization density with distance above the burner top.	43
7	The seeding apparatus.	45

FIGURE		PAGE
8	The structure of grid	47
9	The grid current as a function of grid voltage measured at a distance of 10 cm from the top of the burner.	50
10	The variation of ion current inside and outside the sheath	52
11	The circuit diagram for the measurement of space potential and ionization density in the flame.	53
12(a)	The current voltage characteristics of a cylindrical probe. The solid line shows the theoretical probe current according to equation (24) and the circles are the experimental probe current at density $n_o = 1.7 \times 10^{12}/m^3$.	57
12(b)	The current voltage characteristics of a cylindrical probe. The solid line shows the theoretical probe current according to equation (24) and the circles are the experimental probe current at density $n_o = 1.7 \times 10^{13}/m^3$.	58

FIGURE PAGE

13 The variation of electric field inside and outside the sheath 60

14 The transition from sheath/convection to field limited current of a cylindrical probe is shown with the variation of $\frac{R_e^{\alpha}}{\sqrt{x}}$ 61

● - Clements and Smy from ref-21.

■ - In plasma at the top of the chimney

▲ - Inside the sheath.

The horizontal solid line is calculated from the sheath/convection theory and the solid sloping line is from field limited current theory.

CHAPTER I

INTRODUCTION

The development of accurate, well understood plasma diagnostic techniques (i.e. determination of plasma characteristics, mainly electron and ion density, electron temperature, recombination rate etc.) is essential in plasma research. Any progress in the understanding of naturally occurring plasmas or in utilizing existing techniques in the production of plasma will put this science another step ahead. Primary sources of naturally occurring plasma include the ionosphere and flame plasmas.

1.1 FLAME AS A PLASMA SOURCE

The convenience of the production of flames makes them a very important source of plasma. They have a temperature range from $1000^{\circ}K$ to $4000^{\circ}K$ and a pressure range of typically from 1 torr to 100 atmospheres. The electron concentration of a flame can vary from $10^{12}/m^3$ to $10^{20}/m^3$ with Debye shielding lengths of the order of 3×10^{-6} to 3×10^{-4}m. The usual characteristic flame dimensions of 10^{-2} to 10^{-1}m. are sufficient to allow the flame to be treated as a true plasma as distinct from a simple ensemble of ions and electrons. The collision frequency of electrons and neutral molecules in flame gases is of the order of $\nu = 10^{-13}$ [M]/sec where[M] = Concentration of neutral molecules per meter^3.

In an atmospheric pressure flame $\nu \approx 3 \times 10^{11}/\text{sec}$[1]. Because of these qualities research workers have used flames as a convenient source of plasma for many experiments.

Various techniques have so far been proposed for the study of flame plasmas namely,

1. Microwaves
2. Electrostatic Probes
3. Mass Spectrometry
4. Spectrophotometry
5. Electron Cyclotron Resonance
6. Radio Frequency Coils

The first three methods have met with a good deal of success.

The microwave method[2] suffers from a drawback because it needs space to place the flame within the cavity. The spatial resolution is thus reduced by the presence of large holes in the cavity walls. The holes in the cavity which are necessary for the entrance and exit of the hot flame gases also permit the electric and magnetic fields to leak out of the cavity.

The limitations of the mass spectrometer are associated with the problem of accurate sampling of the flame gases. Although much work has been done to alleviate the problem,

it is at its worst at high gas pressures and extreme care must be taken in identifying true flame ions.

1.2 ELECTROSTATIC PROBE AS A PLASMA DIAGNOSTIC

Electrostatic probes are one of the fundamental techniques in plasma diagnostics. In 1924 Langmuir developed this technique. The probe is a metallic wire inserted into the plasma and biased positive or negative with respect to the plasma with the help of a power supply or battery. The current-voltage characteristics provide information about the condition of the plasma. For a wide range of conditions the presence of the probe does not perturb the plasma. Thus the probe does not have any effect on the quantities being measured. The electrostatic probe offers good spacial resolution over a wide range of conditions. Although the probe is very easy to construct, the interpretation of the results is not so simple. The difficulty arises because probes are boundaries to the plasma. The governing equations of motion of the charged particles in the plasma do not hold in the boundary region. The condition of quasineutrality which is true for the plasma is not valid near the boundary (which is known as a "sheath") where the electron and ion density differ.

Langmuir and H.M. Mott Smith[3] assumed a thin boundary layer around the probe and noted that the quasineutral

equation could be used up to the 'sheath edge' which in practice had a well-defined position.

In recent years scientists have tried to understand the behaviour of a probe in a high pressure plasma. Schultz and Brown[4] tried to interpret the positive ion saturation region of a probe at low pressure, taking into account the directed current at the sheath edge. Good agreement was found between the theoretical and experimental results at low pressure. At high pressure the probe collects about twice the current predicted by the theory. Their theory was based on the assumption of a sheath region around the probe. Su and Lam[5] have presented a continuum theory for a negatively biased probe in a slightly ionized high neutral density gas. They assumed a slightly ionized plasma, which was quiescent. They have given two explicit forms of current-voltage characteristics, one for very negative probes and the other for probes at close to plasma potential. Both of these are based on the assumption that the probe radius is large compared to the Debye length. Soundy and Williams[2] developed a probing technique along the lines suggested by the theory of Su and Lam, but the current collected by the probe was 100 times greater than the theoretically predicted current. A number of theories have been put forward to explain this dis-

crepancy.

1.3 ELECTROSTATIC PROBE FOR THE DIAGNOSTICS OF FLOWING PLASMAS

It has been found experimentally that the electrostatic probe theory works satisfactorily in static plasmas. However, the theory does not work in most atmospheric plasmas since in fact such plasmas must usually be considered as moving plasmas, because of their inherent motion. There has been considerable interest in the application of probe theory in this type of moving plasma[6-12].

Lam[6] first looked into the case of high pressure moving plasmas For a probe, the condition of ion collection reduced to that considered by Su and Lam for the case of electric Reynolds number $R_e << 1$, where the electron and ion temperature are approximately the same.

$$R_e = 2v_f r_p D_i^{-1}$$

where

v_f = plasma convection velocity

r_p = probe radius

D_i^{-1} = positive ion diffusivity

This theory is only applicable under the following conditions:

1. The mean free path of the charged particles is

much smaller than the thickness of the sheath.

2. The Debye length is much smaller than the thickness of the boundary layer adjacent to the body surface.

The prediction of Lam was that the probe acts as a sink to the charged particles which lose their charge by recombining on the surface of the probe. The electrons will hit the probe more often than the heavier ions due to their large thermal velocity. Immediately next to the body surface the number density of electrons becomes too low to carry the ions and the ions' own diffusion motion takes over. Outside this ambipolar diffusion region, convection effects are dominant and the electron and ion densities are uniform and equal.

De Boer and Johnson[13] have derived the sheath thickness and current collected by the probe which depends on the conservation of ions entering the sheath from the free stream. They have assumed that the boundary layer between the quasineutral region and the sheath edge is very small. A strong electric field acts at the ion sheath and the effect of the electric field on the ion flow is very small. The free stream electric field cannot be precisely zero, since some field strength is required to drive the electron towards the positive electrode. The ions having been

convected through the sheath edge are assumed to change direction abruptly and then move directly to the probe, under the influence of strong electric fields, in the sheath. Again since the plasma is flowing, a hydrodynamic boundary layer is formed around the probe. If the electric sheath is much thicker than this hydrodynamic boundary layer, convection within the sheath may be neglected[14]. The mechanism of ion flow within the sheath can be treated as one dimensional, which greatly simplifies the task of solving the sheath equation. At low ion density the sheath becomes thick compared to the hydrodynamic boundary layer. For sufficiently low ion density, the sheath can fill a hollow probe, which then serves as a total collector of all ions convected into its entrance area. In describing the motion of ions in a sheath, De Boer[14] concluded that convection simply adds a constant horizontal component to the ion motion in the major part of the sheath. The predominant electric effect is in the vertical direction and not in the horizontal direction, but the electron density from probe measurement was 50% more in De Boer measurement.

Clements and Smy divided the high pressure moving probe theory into two regions namely, $R_e\alpha^2x^2 >> 1$ and $R_e\alpha^2x^2 << 1$ where R_e = electric Reynolds number

$$\alpha^2 = \frac{\varepsilon_o kT_e}{n_e e^2 r_p^2}$$

ε_o = Permittivity of free space

k = Boltzman's constant

T_e = Electron temperature

n_e = Electron density

e = Electronic charge

r_p = Probe radius

$x = eV/kT_e$

V = Probe potential (negative)

μ_i = Ionic mobility

For $R_e \alpha^2 x^2 >> 1$ Clements and Smy have shown that the supply of ions to a negatively biased probe arises predominantly from hydrodynamic convection of ions into the probe sheath. If the sheath remains thin compared to the probe radius, the theoretical current per unit length to a cylindrical probe is [15],

$$I = 5.3(n_e e v_f)^{3/4} V^{1/2} (\mu_i \varepsilon_o r_p)^{1/4}$$

For $R_e \alpha^2 x^2 << 1$, the supply of ions to the probe is governed by diffusion of ions through the electric boundary layer surrounding the probe. The theoretical diffusive current per unit length to a cylindrical probe was derived as [16],

$$I_d = 4(e\mu r_p v_f kT_e)^{1/2} n_e$$

By following the guide lines presented by Lam, Clements and Smy [16] came up with a simple expression for the transition between diffusive and sheath convective behaviour in the absence of recombination. They found this transition to be a reasonably broad one, which in fact covers a range of about two orders of magnitude of the variable $(R_e \alpha^2 x^2)^{1/4}$. Additional complications arise from the cold dense gases in the hydrodynamic boundary layer. When this boundary layer is thick in comparision with the sheath, then the boundary layer resistance has a large influence on the probe current.

1.4 THE NATURE OF THE PRESENT WORK

There is no definite theory to calculate the electron density from the saturation ion current under a variety of plasma conditions. The dominant supply of ions to a negative probe arises from their convection or diffusion into the sheath surrounding the probe. In the simple model proposed by De Boer and Johnson [13], Kulgein [17], Clements and Smy [15] the ions had been convected through the sheath edge. Once they cross the sheath edge, the ions change direction quickly under the influence of the high electric field which occurs in the sheath and move towards the probe. This theory has been applied by others

to different probes (cylindrical, spherical, and stagnation probe) and sheath configurations (planar, cylindrical). Good agreement has been found with existing experimental data for ionization densities in the range of 10^{15} - $10^{21}/m^3$. The sheath convection theory gives good agreement, but a significant error arises in the case of sheath-diffusion theory (De Boer[13] ∿10x, Clements and Smy[18] ∿100x). This particular mode of operation, the so called sheath/convection mode, is particulary desirable because for many geometries the theory is simple; its assumptions are reasonably well satisfied and the measurement is performed on an 'undisturbed plasma', since the sheath edge which abstracts ions from the plasma extends beyond the hydrodynamic and thermal boundary layers surrounding the probe. As has been pointed out above, the application of the sheath/convection model is limited by various parameters. This thesis describes an experimental investigation of probe behaviour at ionization densities down to $10^{12}/m^3$ in a region where the sheath/convection model loses validity and therefore another model must be used. The theory developed for this new region of ultra-low ionization densities (for laboratory plasmas) also is shown to have application to the measurement of ion densities within thick sheaths or clouds of positive ions.

Hoult[19] and Sonin[20] have developed a theory for the blunt nosed probe which has some similarity with the present theory. Their theory does not consider cylindrical or spherical geometry and takes no account of the sheath effects. The experimental measurement shows good agreement with the theory presented here.

CHAPTER II

THEORY

2.1 THE LIMIT OF SPACE CHARGE AND FIELD LIMITED CURRENT

The simple sheath/convection model by De Boer and Johnson[13], and Clements and Smy[21] is shown in fig. (1). In the case of a cylindrical probe in atmospheric plasmas, the sheath radius is much greater than the probe radius. The essential point of the sheath/convection model is that all ions convected into the sheath eventually arrive at the probe due to the strong electric field in the sheath. The field $E \simeq 0$ at the sheath edge (the boundary of the plasma electrons), and as soon as the ions enter into the sheath their motions are determined by the sheath electric field. The sheath radius then adjusts to such a value (r_o) (assuming a cylindrical symmetry) that the current to the probe is space charge controlled. The ion current/unit length at a distance r is given by

$$i = -2\pi r n_e \mu_i E e \qquad (1)$$

where μ_i = ion mobility, E = the electric field of the probe, e = electronic charge, n_e = ionization density.

From Poisson's equation, in cylindrical coordinates

$$\frac{d^2V}{dr^2} + \frac{1}{r}\frac{dV}{dr} = -i(2\pi\, r\mu_i\varepsilon_o(dV/dr))^{-1} \qquad (2)$$

Schultz and Brown[4] have integrated this equation applying the boundary condition E=V=0 at $r = r_o$ and $V = V_p$ at $r = r_p$ and $i = I$ giving rise to the expression

$$I = \frac{2\pi\mu_i\varepsilon_o V_p^2 r_p^{-1}}{\frac{r_o^2}{r_p^2}\left[\log(r_o/r_p)\right]^2} \qquad (3)$$

where ε_o = Permittivity of free space.

It is noted that in deriving the asymptotic expression above, a factor of 1.37 in the 'log' term has been neglected for simplicity. The supply of ions to the outer edge of the sheath will now be generated by convection for $r_o >> r_p$ and $R_e > 1$ and will consequently be given by

$$I = 2r_o n_e e v_f \qquad (4)$$

R_e = electric Reynold's number = $2v_f r_p/\mu_i kT_e/e$

v_f = flow velocity of the plasma,

k = Boltzman's constant

T_e = electron temperature.

It is apparent from equations (3) and (4) that the sheath

thickness r_o will adjust so that the linear convection of ions into the sheath is just balanced by the radial space charge limited flow of ions into the probe. Eliminating r_o from equations (3) and (4) Clements and Smy[21] obtained

$$V = \frac{I^{3/2}}{(2\pi\mu_i\varepsilon_o)^{1/2}(2n_e e v_f)} \log\left(\frac{I}{2n_e e v_f r_p}\right)$$

$$I = \frac{(2\pi\mu_i\varepsilon_o)^{1/3}(2en_e v_f V)^{2/3}}{\left[\log\left(\frac{I}{2n_e e v_f r_p}\right)\right]^{2/3}} \qquad (5)$$

At low ionization density or at high flow velocity it is observed that the fields within the sheath may not be strong enough to ensure that a large portion of the ions entering the sheath do indeed reach the probe; many, in fact, will be swept on by the flow back into the plasma. This situation is indicated in fig. (1-b). The ions between AA will only contribute to the probe current, the others will not contribute to the probe current although they remain in the sheath for a period of time. It can be decided which of these regions best describes a given

probe situation by considering the situation (1-b), in this case the motion of most ions within the sheath is largely unaffected by the sheath electric field. Consequently, the ion density remains close to the value in the plasma and with a cylindrical sheath of radius 'r_o' with potential 'V' we have

$$2\pi r\varepsilon_o E = \pi r^2 n_o e \qquad \text{where } r_o >> r_p$$

$$E = \frac{r n_o e}{2\varepsilon_o} = -\frac{dV}{dr}$$

$$V = \frac{r_o^2 n_o e}{4\varepsilon_o} \tag{6}$$

The sheath electric field then can be calculated and is given by

$$V^2 = \frac{r_o^2 n_o e V}{4\varepsilon_o}$$

$$\left(\frac{V}{r_o}\right)^2 = \frac{n_o e V}{4\varepsilon_o}$$

$$\frac{V}{r_o} = \sqrt{\frac{n_o e V}{4\varepsilon_o}} \tag{7}$$

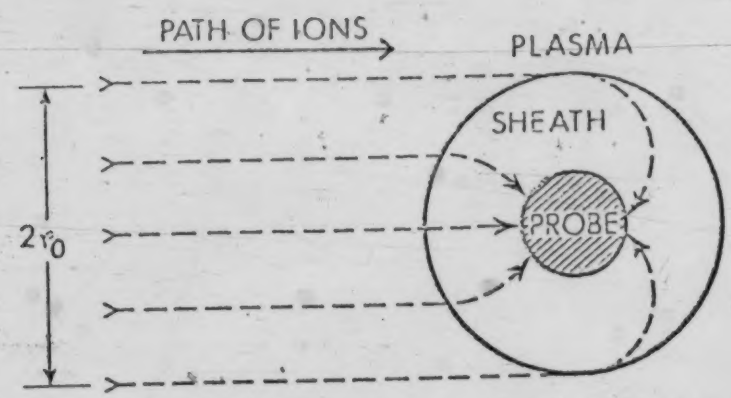

FIGURE (1-a) Sheath/convection model from ref-22. All ions convected into the sheath eventually arrive at the probe.

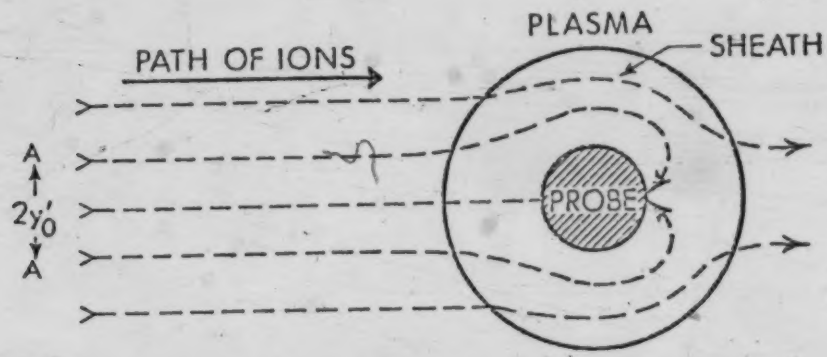

FIGURE (1-b) Field limited model. Only the ions in the band AA reach the probe.

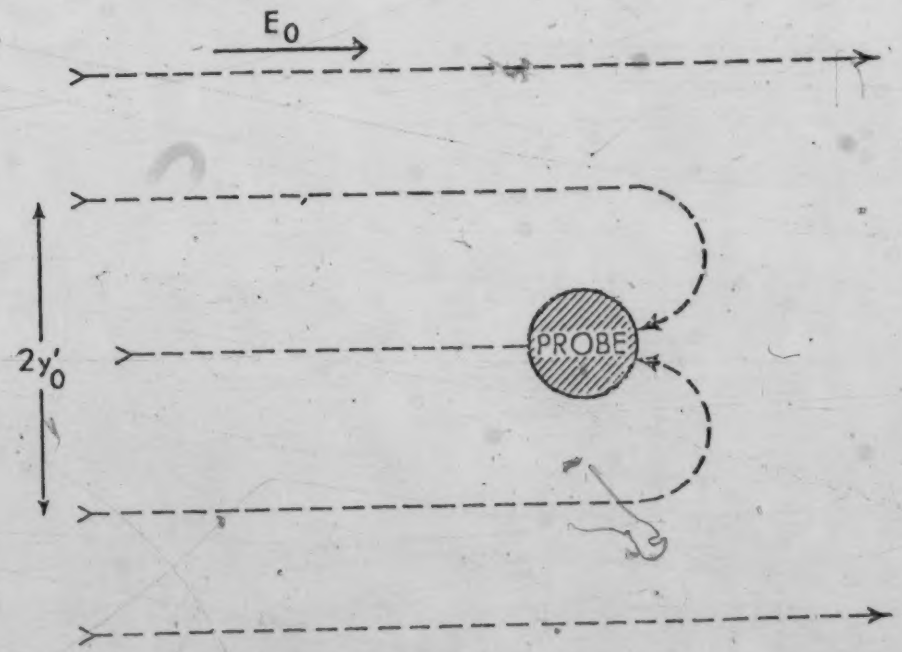

FIGURE (1-c) Planar sheath model. Eo is the local field.

It is noted that the assumption of the ion motion will hold if the product of this electric field and the ion mobility $\ll$ ion convection velocity.

$$\mu_i E << v_f$$

$$\mu_i \sqrt{\frac{Vn_o e}{4_o}} << v_f \tag{8}$$

Converting the equation (8) into non-dimensional parameters in terms of R_e, $\alpha = \sqrt{\frac{\varepsilon_o kT_e}{n_o e^2}} \frac{1}{r_p}$ and $x = \frac{eV}{kT_e}$

$$\frac{v_f}{\mu_i \sqrt{\frac{Vn_o e}{4\varepsilon_o}}} >> 1$$

$$\frac{R_e \alpha}{\sqrt{x}} >> 1 \tag{9}$$

Thus, it is found that if $\frac{R_e \alpha}{\sqrt{x}} << 1$, the current is space charge limited and if $\frac{R_e \alpha}{\sqrt{x}} >> 1$, the current is not space charge limited.

2.2 THIN PROBE CYLINDRICAL GEOMETRY

If the motion of most of the ions within the sheath is not affected very much by the sheath electric field, then the ionization density everywhere in the sheath apart from the region close to the probe will be uniform and equal to the ion density in the plasma.

Let Q be the charge per unit length on the probe, which is equal and opposite to the total charge of the ions in the sheath. The electric field in the region close to the probe will be given by the expression

$$\underline{E} = \frac{Q}{2\pi\varepsilon_o r}\hat{r} \tag{10}$$

where $\hat{r}$ is the unit radius vector to the probe. This region is the most important region, since it is only from this region that ions can be removed from the gas.

If an ion moves with velocity vector $\underline{v}$ relative to the probe and the velocity of gas relative to the probe is $\underline{v}_f$ then the velocity of the ion relative to the gas is $(\underline{v} - \underline{v}_f)$, and which has been produced by an electric field

$$\underline{E} = \frac{1}{\mu_i}(\underline{v} - \underline{v}_f) \tag{11}$$

From equation (10) we have

$$\underline{E} = \frac{Q}{2\pi\varepsilon_o r}\,\hat{r} = \frac{1}{\mu_i}(\underline{v} - \underline{v}_f)$$

Thus the path of an ion relative to the probe is described by the velocity vector

$$\underline{v} = \underline{v}_f + \frac{Q\mu_i \hat{r}}{2\pi\varepsilon_o r} \qquad (12)$$

We can convert the equation (12) in terms of the non-dimensional quantities using $X = \frac{x 2\pi\varepsilon_o v_f}{Q\mu_i}$, and $Y = \frac{y 2\pi\varepsilon_o v_f}{Q\mu_i}$, where x and y are the co-ordinates parallel and perpendicular to $\underline{v}_f$ respectively, with the origin at the probe.

Thus the component of $\underline{v}$ in the y-direction, from fig (1-d), is

$$v_y = \frac{dy}{dt} = \frac{Q\mu_i}{2\pi\varepsilon_o r}\sin\theta$$

$$= \frac{Q\mu_i}{2\pi\varepsilon_o r^2} r\sin\theta$$

$$= \frac{Q\mu_i\, y}{2\pi\varepsilon_o (x^2+y^2)} \qquad (13)$$

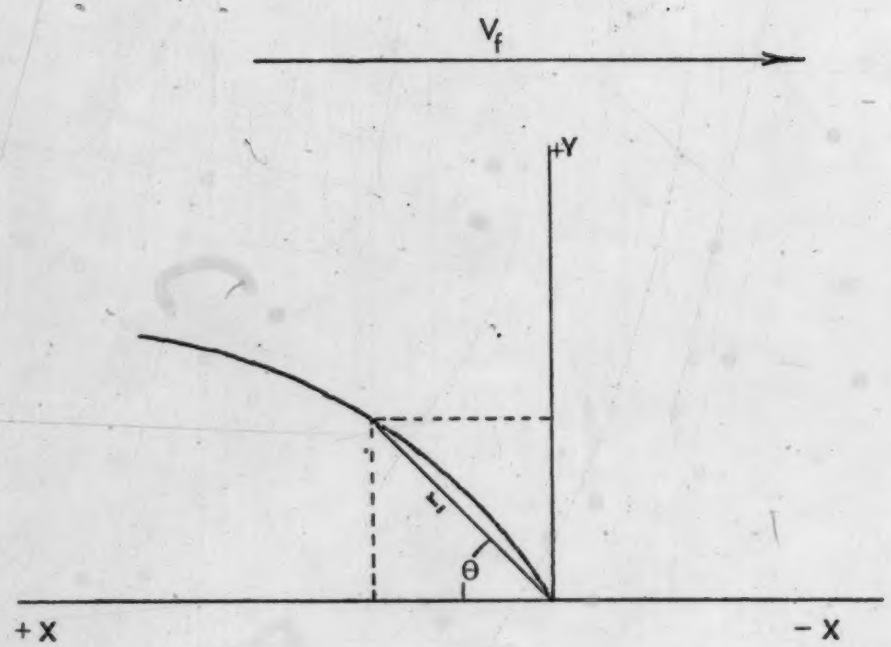

FIGURE (1-d) The co-ordinate system for equations (13) and (14).

The component of $\underline{v}$ in the x-direction, from fig (1-d), is

$$v_x = \frac{dx}{dt} = -v_f + \frac{Q\mu_i}{2\pi\varepsilon_o r}\cos\theta$$

$$= -v_f + \frac{Q\mu_i}{2\pi\varepsilon_o r^2}\, r\cos\theta$$

$$= -v_f + \frac{Q\mu_i}{2\pi\varepsilon_o (x^2+y^2)}\, x \qquad (14)$$

From equations (13) and (14) one gets

$$\frac{dy}{dx} = \frac{\dfrac{Q\mu_i y}{2\pi\varepsilon_o (x^2+y^2)}}{\dfrac{Q\mu_i x}{2\pi\varepsilon_o (x^2+y^2)} - v_f}$$

$$= \frac{y}{x - \dfrac{2\pi\varepsilon_o v_f (x^2+y^2)}{Q\mu_i}}$$

$$\frac{dY}{dX} = \frac{\dfrac{Q\mu_i}{2\pi\varepsilon_o v_f}\, Y}{\dfrac{Q\mu_i}{2\pi\varepsilon_o v_f}\, X - \dfrac{Q\mu_i}{2\pi\varepsilon_o v_f}\, (X^2+Y^2)}$$

$$\frac{dY}{dX} = \frac{Y}{X - (X^2 + Y^2)} \qquad (15)$$

Equation (15) has a solution given by,

$$Y - \tan^{-1} \frac{Y}{X} = \text{Constant} \qquad (16)$$

Plots of this equation appropriate to three different values of the constant are shown in fig.(2). The solid line shows the trajectories of ions whose initial value at $x = -\infty$ is $Y = Y_o'$. The ions whose initial value at $x = -\infty$ is less than Y_o' will finally meet the probe. The ions whose initial values are greater than Y_o' will pass on towards $x = +\infty$. Inspection of equation (16) above shows that this situation occurs when the constant = 0

$$Y = \tan^{-1} \frac{Y}{X} \quad \text{and at} \quad Y = 0 \quad X = 1$$

$$\tan Y_o' = 0 \qquad Y_o' = \pi \qquad (17)$$

Only those ions having the value of $Y_o' \geq Y \geq -Y_o'$ at $x = -\infty$ will reach the probe, and thus the ion current/unit length of probe within the band $Y = \pm Y_o'$ will be

$$I_p = n_o e v_f A \qquad \text{where A = area}$$

$$= n_o e v_f 2y_o' \qquad (18)$$

$$\text{where} \quad y_o' = \frac{Q \mu_i Y_o'}{2\pi\varepsilon_o v_f} \qquad (19)$$

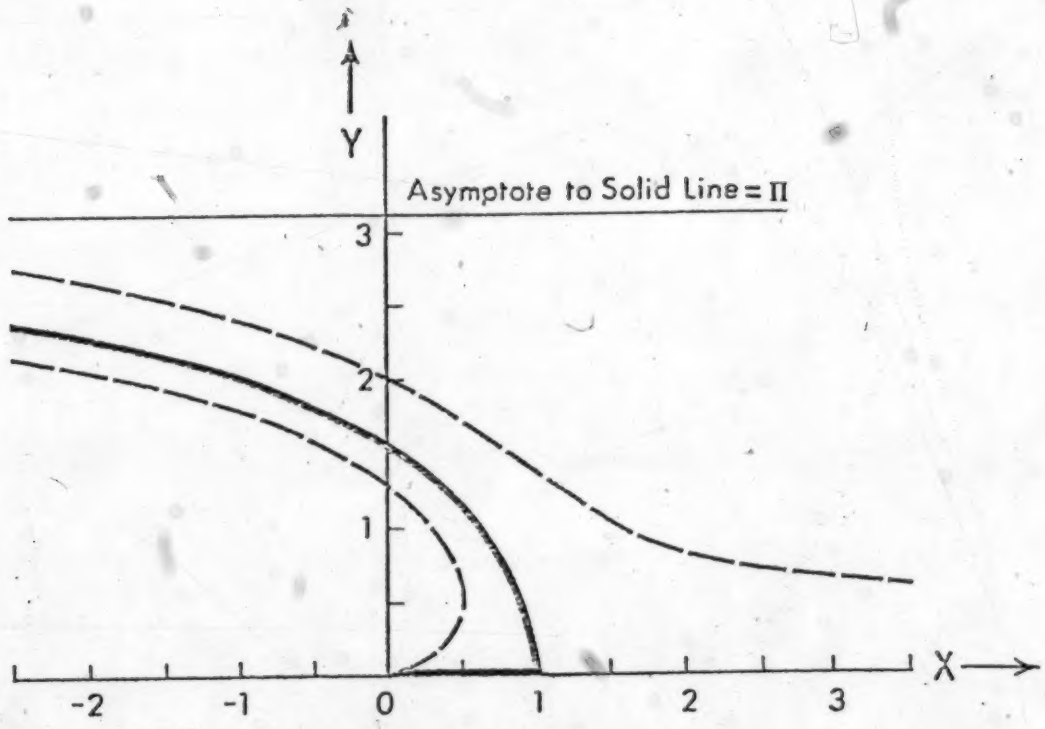

$$\frac{dY}{dX} = \frac{Y}{X - X^2 - Y^2}$$

The Boundary Conditions are at $X = 1, Y = 0$

$$\frac{dY}{dX} = \infty$$

FIGURE (2) The trajectories for ions having different impact parameters solved from equation (15).

$$I_p = n_o e v_f \frac{2Q\mu_i Y_o'}{2\pi\varepsilon_o v_f}$$

$$= \frac{n_o e Q \mu_i Y_o'}{\pi\varepsilon_o} \qquad (20)$$

But at $x = -\infty$, $Y_o' = \pi$

Therefore the ion current/unit length is

$$I_p = \frac{n_o e Q \mu_i}{\varepsilon_o} \qquad (21)$$

To obtain a current-voltage relation for such a probe it remains to relate the charge Q to the voltage applied to the probe. In the basic model we assumed that most of the ions within the sheath were essentially unaffected by the probe. Thus, for the purposes of calculating the probe voltage the sheath can be considered as a cylinder of radius r_o uniformly filled with a charge density of $n_o e$ with no electric field or potential at its surface.

The negative charge on the probe will be equal and opposite to the positive charge in the sheath. We see that the charge Q on the probe will be $\simeq -\pi r_o^2 n_o e$ which together with the volume charge of the sheath will produce an electric field at any point $\underline{r}$ in

the sheath is

$$\frac{dV}{dr} = - \frac{(r_o^2 - r^2) n_o e}{2\varepsilon_o r}$$

Integrating the above equation one gets

$$V = - \frac{n_o e r_p^2}{2\varepsilon_o} \left(\frac{r_o^2}{r_p^2} \log \frac{r_o}{r_p} - \frac{r_o^2 - r_p^2}{2r_p^2} \right) \qquad (22)$$

For the experimental range of $3 > \log \frac{r_o}{r_p} > 1.2$ the quantity in brackets in equation (22) can be approximated by $\frac{1}{5} \left(\frac{r_o}{r_p}\right)^{2.8}$

$$V = \frac{e n_o r_p^2}{2\varepsilon_o} \frac{1}{5} \left(\frac{r_o}{r_p}\right)^{2.8}$$

$$r_o^2 = \left(\frac{10 \varepsilon_o V r_p^{2.8}}{e n_o r_p^2} \right)^{2/2.8}$$

But $Q = \pi e n_o r_o^2$

$$= \pi e n_o \left(\frac{10 \varepsilon_o V r_p^{2.8}}{e n_o r_p^2} \right)^{2/2.8} \qquad (23)$$

But from equation (21) we get

$$I_p = \frac{Q \mu_i e n_o}{\varepsilon_o}$$

Putting the value of Q from equation (23) one gets

$$I_p = \frac{en_o\mu_i}{\varepsilon_o} \pi en_o r_p^2 \left(\frac{10\varepsilon_o V}{en_o r_p^2}\right)^{0.7}$$

$$= \pi e\, n_o \mu_i V \left(\frac{215 en_o r_p^2}{\varepsilon_o V}\right)^{0.3}$$

$$= 2\,\pi en_o\mu_i V \left(\frac{21.33 en_o r_p^2}{\varepsilon_o V}\right)^{0.3} \qquad (24)$$

Again, from equation (22) we get

$$V = -\frac{n_o e r_p^2}{2\varepsilon_o}\left(\frac{r_o^2}{r_p^2}\log\frac{r_o}{r_p} - \frac{r_o^2 - r_p^2}{2r_p^2}\right),$$

$$= -\frac{n_o e r_o^2}{2\varepsilon_o}\left(\log\frac{r_o}{r_p} - \frac{r_o^2 - r_p^2}{2r_o^2}\right)$$

But $Q = -\pi r_o^2 n_o e$

$$V = \frac{Q}{2\pi\varepsilon_o}\left(\log\frac{r_o}{r_p} - \frac{1}{2} + \frac{r_p^2}{2r_o^2}\right)$$

since $r_o >> r_p$.

$$V = \frac{Q}{2\pi\varepsilon_o}\left(\log\frac{r_o}{r_p} - \frac{1}{2}\right)$$

$$Q = \frac{2\pi\varepsilon_o V}{\log \frac{r_o}{r_p} - \frac{1}{2}} \qquad (25)$$

Putting the value of Q in equation (21) one gets

$$I_p = \frac{2\pi e n_o \mu_i V}{\log \frac{r_o}{r_p} - \frac{1}{2}}, \qquad (26)$$

2.3 THICK PROBE CYLINDRICAL GEOMETRY

With high flow velocities or with large diameter probes the distance Y_o' becomes very small compared to the probe radius. In this case, flow is different. The electric field, equal to $\frac{Q}{2\pi\varepsilon_o r}$, will be constant while the flow velocity considering the inviscid flow varies with position and is given by

$$v = 2 v_f \sin\phi \qquad (27)$$

where ϕ is the angle between the velocity vector $\underline{v}_f$ and the radius to the point concerned as shown in fig (1-e). The ion moves through an angle $d\phi$ in time dt.

$$\frac{d\phi}{dt} = \frac{2v_f \sin\phi}{r} \qquad (28)$$

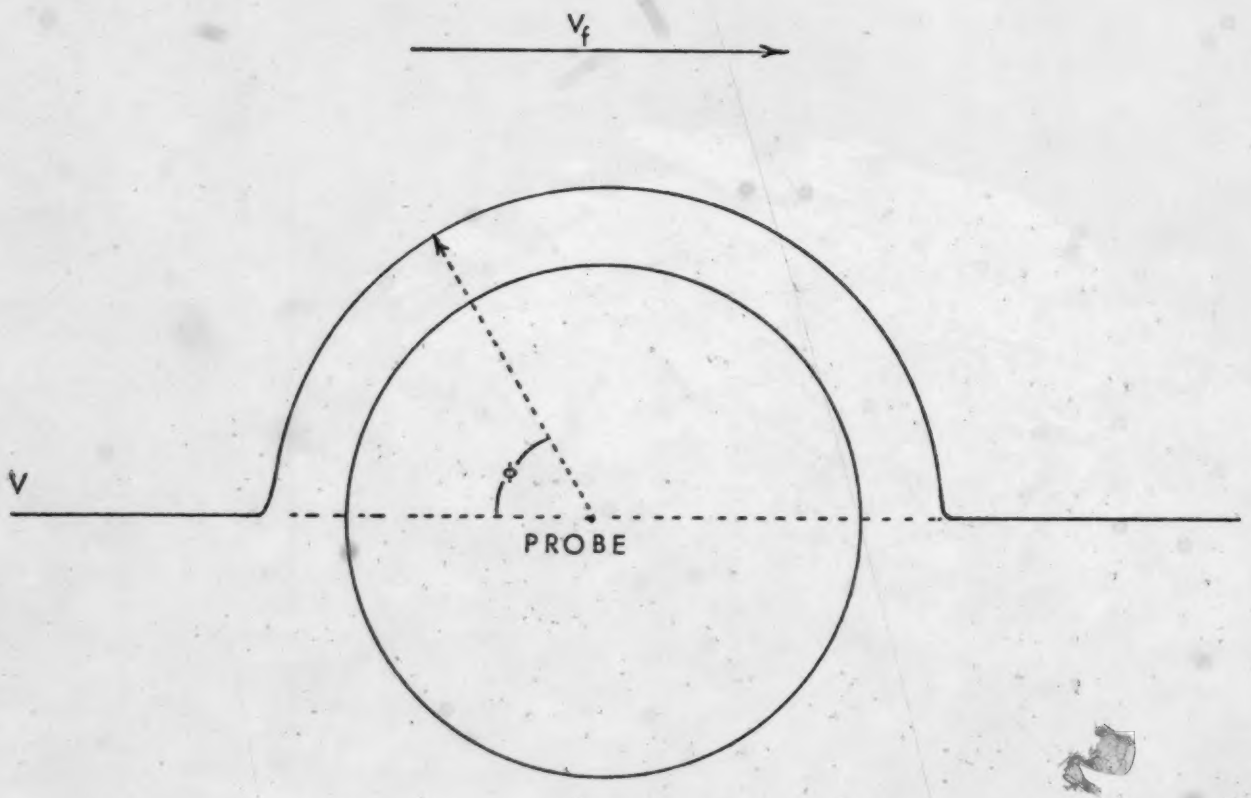

FIGURE (1-6) The trajectories of the particles very close to a probe, due to inviscid flow.

and during this time the ion will move radially inwards under the action of an electric field by an amount dr, therefore,

$$\frac{dr}{dt} = \frac{Q\mu_i}{2\pi\varepsilon_o r}$$

But

$$\frac{dr}{d\phi} = \frac{dr}{dt}\ \frac{dt}{d\phi} = \frac{Q\ \mu_i}{4\pi\varepsilon_o v_f \sin\phi}$$

$$\frac{dr}{d\phi} = \frac{Q\mu_i}{4\pi\varepsilon_o v_f \sin\phi} \qquad (29)$$

Following Clements and Smy[15] in a similar situation involving the sheath convection model, it is necessary to modify equation (25) in the flow and an extra term is to be added for the inherent radial flow velocity. As a result equation (29) becomes

$$\frac{dr}{d\phi} = \frac{Q\mu_i}{4\pi\varepsilon_o v_f \sin\phi} - \frac{y\cos\phi}{\sin\phi}$$

which has the solution

$$r\sin\phi = \frac{Q\mu_i}{4\pi\varepsilon_o v_f} + c \qquad (30)$$

The current/unit length to the probe will be

$$I_p = 2\,(2v_f\, r \sin\phi\, n_o e)_{\phi=o}^{\phi=\pi} = \frac{Q\mu_i n_o e}{\varepsilon_o} \qquad (31)$$

2.4 SPHERICAL PROBE GEOMETRY

In the case of a spherical probe, the inviscid flow velocity which varies with position is given by,

$$v = \frac{3}{2} v_f \sin\phi$$

In time dt, the ion will move through an angle $d\phi$ and during this time will move radially inwards under the action of an electric field. Considering the inherent radial flow velocity in this situation, one gets,

$$\frac{dr}{d\phi} = \frac{Q\mu_i}{4\pi\varepsilon_o r_p} \frac{2}{3v_f \sin\phi} - \frac{2r\cos\phi}{\sin\phi} \qquad (32)$$

$$\sin^2\phi \frac{dr}{d\phi} + 2r \sin\phi \cos\phi = \frac{Q\mu_i}{4\pi\varepsilon_o} \frac{2}{3v_f} \sin\phi$$

$$(r\sin^2\phi) = \frac{Q\mu_i}{4\pi\varepsilon_o r_p} \frac{2}{3v_f} (-\cos\phi) + c$$

The current to the probe is given by,

$$I_p = n_o e v 2\pi \sin\phi\, r\, r_p$$

$$= (n_o e \frac{3}{2} v_f \sin\phi\, 2\pi \sin\phi\, r\, r_p)_{\phi=o}^{\phi=\pi}$$

$$I_p = \frac{n_o e Q \mu_i}{\varepsilon_o} \qquad (34)$$

But, one knows that

$$V = \frac{Q}{4\pi\varepsilon_o r_p}$$

$$Q = 4\pi\varepsilon_o r_p V \qquad (35)$$

Putting the value of Q in equation (34) one gets

$$I = 4\pi e n_o \mu_i r_p V \qquad (36)$$

2.5 PROBE MEASUREMENT IN AN EXTERNALLY GENERATED THICK SHEATH

The motivation for these calculations arose from a somewhat different experimental situation. It is possible to determine the ion density profile by means of measurements with a small probe in a thick planar sheath. This situation is shown in fig. (1-c). In this type of sheath region there are only neutral gas molecules and ions in an electric field. By considering the probe and its bias below its surroundings to be small, the sheath electric field can be considered uniform over the region of influence of the probe and the ion density typified by a value n_o.

The total electric field on an ion is given by

$$\underline{E} = \underline{E}_o + \frac{Q\hat{\underline{r}}}{2\pi\varepsilon_o r}$$

which causes an ion drift velocity of

$$\underline{v}_i = \mu_i \left(\underline{E}_o + \frac{Q\hat{\underline{r}}}{2\pi\varepsilon_o r}\right) \qquad (37)$$

The relation between Q and V for the static sheath is, however, different from that for the flowing plasma. It is assumed that the probe does not affect the boundaries of the sheath and so the usual in 'vacuo' expression applies,

$$V = \frac{Q}{2\pi\varepsilon_o} \log\left(\frac{r_o}{r_p}\right) \qquad (38)$$

where $2r_o$ is the length, typical of the dimensions of the sheath. Putting the value of Q in the equation

$$I_p = \frac{Q\mu_i e n_o}{\varepsilon_o}$$

$$= \frac{e n_o \mu_i 2\pi\varepsilon_o V}{\varepsilon_o \log\left(\frac{r_o}{r_p}\right)}$$

$$= \frac{2\pi e n_o \mu_i V}{\log\left(\frac{r_o}{r_p}\right)} \qquad (39)$$

which is similar to equation (26). The expression for a

spherical probe in a static sheath is the same as equation (36).

In deriving equation (39) we have assumed that the ion current near the probe does not distort the electric field. At high densities such distortion will occur and the current to the probe will be limited by the space charge. Effectively the voltage applied between the probe and its surroundings will drop off across the space charge region and only the ions swept into this region will reach the probe. In this situation equation (5) will apply because of the sheath convection situation.

In this section four expressions for the current to cylindrical and spherical probe under different conditions are derived. These formulas can be applied at lower densities in flowing plasma than before and also can be used to carry out direct measurements of ion density in sheaths. The most important differences between the conventional sheath/convection expressions and these derived expressions are the absence of any dependence on flow velocity.

Physically, the probe can be considered as having two limits on its influence on the plasma. The first (appropriate to the electric field that would exist in vacuo) is dictated by the ratio of drag forces to electric forces,

and the second corresponds to the probe length which determines the actual probe currents. Similarly, it is the smallest of the field limited or sheath/convection current which is appropriate. Comparing the two expressions for the cylindrical current, equation (5) (thick sheath) and equation (26) (field limited), we observe that the ratio

$$\frac{I \text{ (thick sheath)}}{I \text{ (field limited)}} = \frac{(2\pi\mu_i\varepsilon_o)^{1/3}(2en_o v_f V)^{2/3}}{2\pi\, en_o\, \mu_i\, \varepsilon_o V}$$

$$= \frac{1}{(2\pi)^{2/3}} \frac{(\frac{2v_f r_p e}{\mu_i k T_e})^{2/3} \; (\sqrt{\frac{\varepsilon_o k T_e}{n_e e^2}} \cdot \frac{1}{r_p})^{2/3}}{(\sqrt{\frac{eV}{kT_e}})^{2/3}}$$

$$= (\frac{R_e^{\alpha}}{\sqrt{x}})^{2/3} \qquad (40)$$

and so we might expect from the discussion leading to relationship (9) that $\frac{R_e^{\alpha}}{\sqrt{x}}$ would define an approximate boundary between the field limited and sheath/convection regimes.

CHAPTER III

EXPERIMENT

INTRODUCTION:

An experimental investigation has been carried out to prove that at low ionization densities the probe current is no longer space charge limited but is, in fact, limited by the electric field generated by the probe. A Meker type of burner was used to produce a high pressure flowing plasma by burning propane and air. Potassium, an alkali material, was used to increase the ionization level in the flame. The current, which gave information about the condition of the plasma, was collected through an air cooled brass probe. An air cooled grid was used to create a planar sheath in the plasma. The flow velocity and the temperature of the flame were measured to scale the mobility of ions. The details of the experiments and their setup are described in different sections of this chapter.

3.1 THE BURNER SYSTEM

The flame is the source of plasma in the exper-

iment. The Meker burner, which produces a uniform and stable plasma, has a small nozzle shaped orifice of 1.5 mm diameter for the gas with an air inlet located just above this orifice. The air is mixed with the gas in a long burner tube before combustion. The long burner tube reduces the turbulence due to the gas jet that is flowing through the burner. The optimal ratio of length to diameter of the burner should be 6:1, whereas the ratio used in the experimental burner is 5:1. The Meker burner used in our experiment gives improved air flow and so achieves a higher temperature and better ionization [22]. The metal grid at the top of the burner prevents flashback and thus achieves a more stable flame. The size of the holes in the grid is not very critical, although a large hole size may increase the risk of flashback. If the holes are too small and close to each other, there is a tendency for the normally separated flames to fuse together and lift off the grid surface to give a conventional bunsen shaped cone. The central apertures in the grid give slightly different combustion conditions, due to the lack of secondary air reaching that region. The grid also acts as a heat sink. Grid

supported flames show much better stability[23] owing to the damping effect which the screen sink has on the front movement of the flame.

Although the front movement of the flames is reduced by the grid it is still the major problem in the burner system. The flame also moves about due to the poor flow regulation. The problem of oscillation of the flame is reduced to a great extent by the grid. The vibrationaly induced eddies can be eliminated by a fixed platform. The instability of a rising hot gas column is responsible for the flickering in the tip of the flame. It is best alleviated by introducing a chimney which captures the hot gas column before the instability develops. This provides a reference hot boundary and adds to the stability of the flame.

The experimental setup of the burner is shown in fig. (3). The high pressure propane passed through a regulating bulb to a propane tank of 3" diameter and 12" length. The propane entered through the bottom inlet and came out from the top. The tank helped keeping a continuous and steady flow of propane to the burner. The gas then enters the burner through a small orifice at the bottom and wasregulated with a flow meter placed in between the tank and the burner. Air is

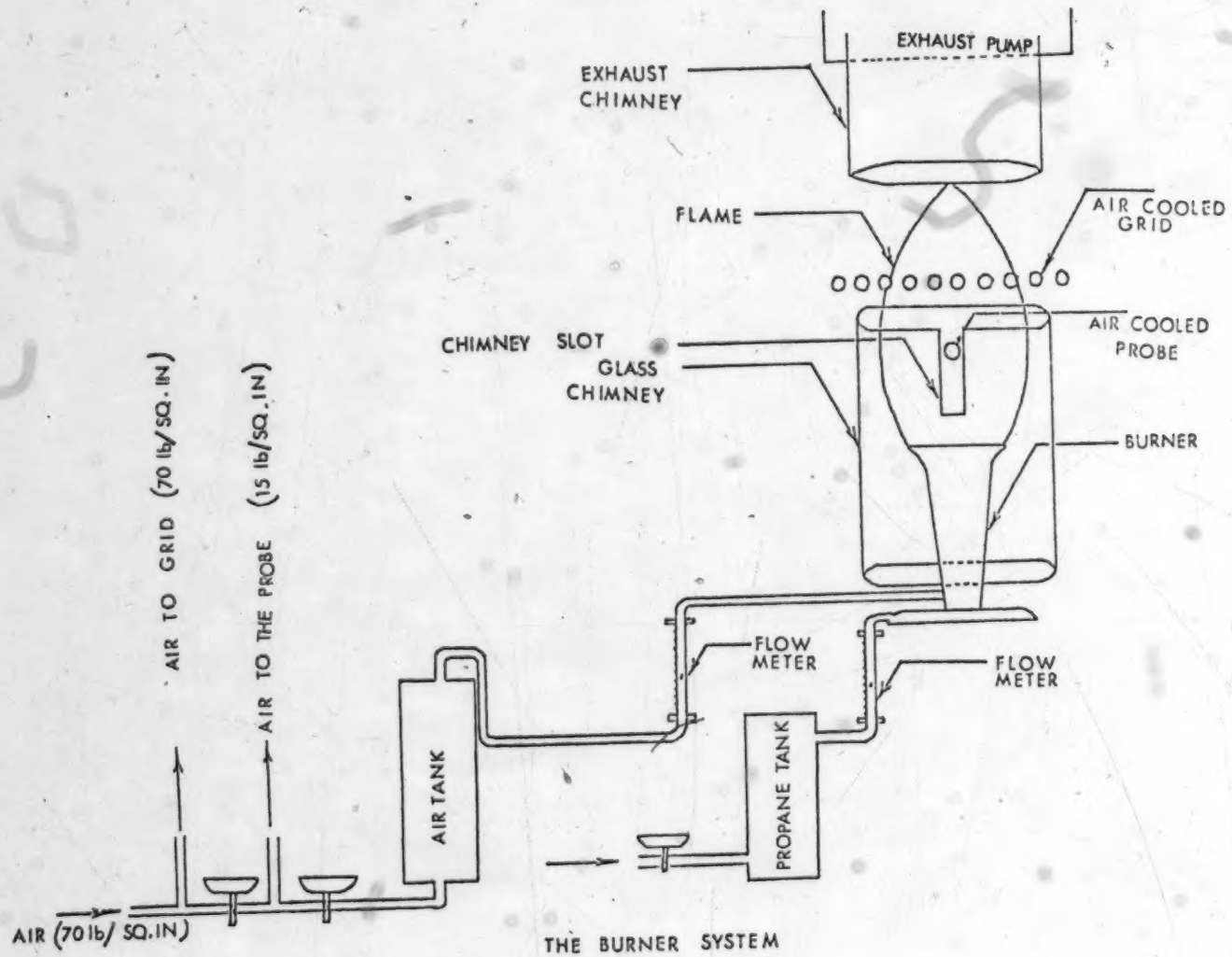

THE BURNER SYSTEM

FIGURE(3)

also passed to the burner through two pressure regulating valves, an air tank and a flow meter. Two chimneys are placed at the top and at the bottom parts of the flame using clamps. It was found experimentally that the chimney at the bottom is the most effective in keeping the flame stable. Photographs of the flame without a chimney, with a chimney at the top and also at the bottom are shown in figs. (4) and (5). The function of the exhause pump at the top is to pump out the burned gases.

3.2 FLAME IONIZATION

It has been found that the most important charged species present in flames are electrons and corresponding amounts of positive ions. There are also small traces of negative ions in flames[24]. The concentration of ions found in the reaction zones of unseeded premixed hydrocarbon/air flames at pressure between 2 to 760 mm Hg lies in the range of 10^{15} - $10^{18}/m^3$[25-28]. The only ions common to all hydrocarbon flames are CH_3^+, $C_3H_3^+$, CHO^+, and H_3O^+. Of these, H_3O^+ is found later than the others and therefore is unlikely to be a primary ion[22]. In the case of the premixed flame, the rate of ion generation increases steeply with final flame temperature (typically by 200% per 100° C). The rate of ion generation also varies with the air/fuel ratio and is a maximum at the stiochiometric ratio. The ion

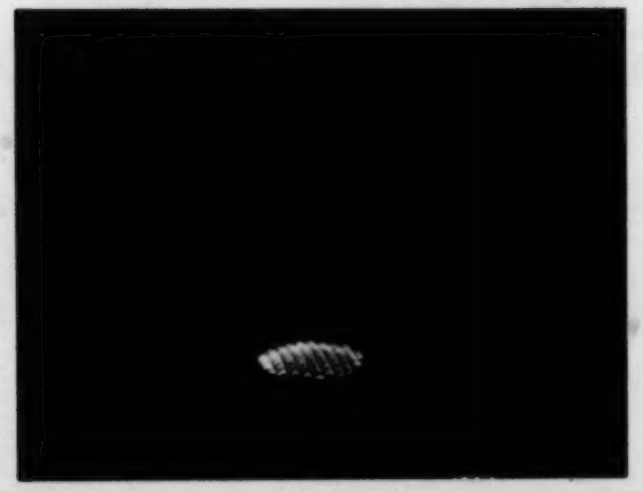

WITH CHIMNEY AT THE TOP OF THE FLAME

FLAME WITHOUT A CHIMNEY

FIGURE(4)

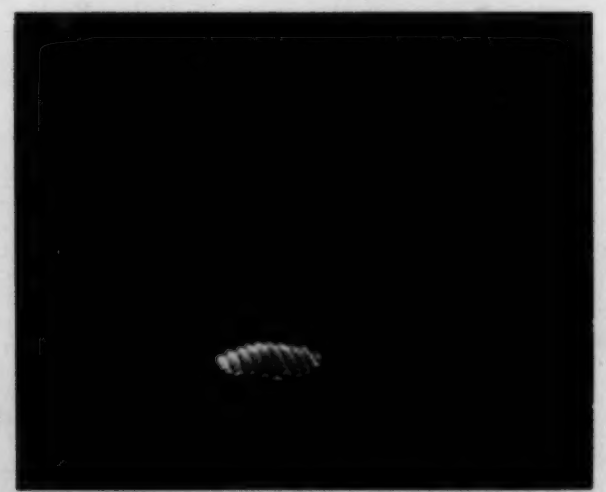

WITH CHIMNEY AT THE BOTTOM
OF THE FLAME

FIGURE(5)

concentration of a propane/air flame is found to vary with pressure and is a maximum at atmospheric pressure[28]. The thickness of the reaction zone of the flame depends on pressure and is a minimum at atmospheric pressure[29]. Clements and Smy[18] found that in a propane/air flame, the ionization is maximum at the reaction zone and falls with distance from the reaction zone. The experimental measurement shown in fig.(6) agrees with the results of Clements and Smy[18]. The experimental measurements were carried out in the range of 2 cms to 10 cms from the top of the burner and it was observed that the ionization remains fairly constant in that region.

3.3 IONIZATION IN THE PRESENCE OF ADDITIVES

The ionization level of flames can be increased by adding small traces of substances having low ionization potential. The rate of ionization in flames is found to be a decreasing function of ionization potential Li<Na<K<Rb<Cs.

The positive ions produced (together with electrons) tend to consist of simple molecular compounds, and are often monoatomic metal ions. Consequently, the corresponding thermal data (ionization potentials) are known. It is also easy to add nebulized solutions of metal salt to the gas supply and to vary these over wide

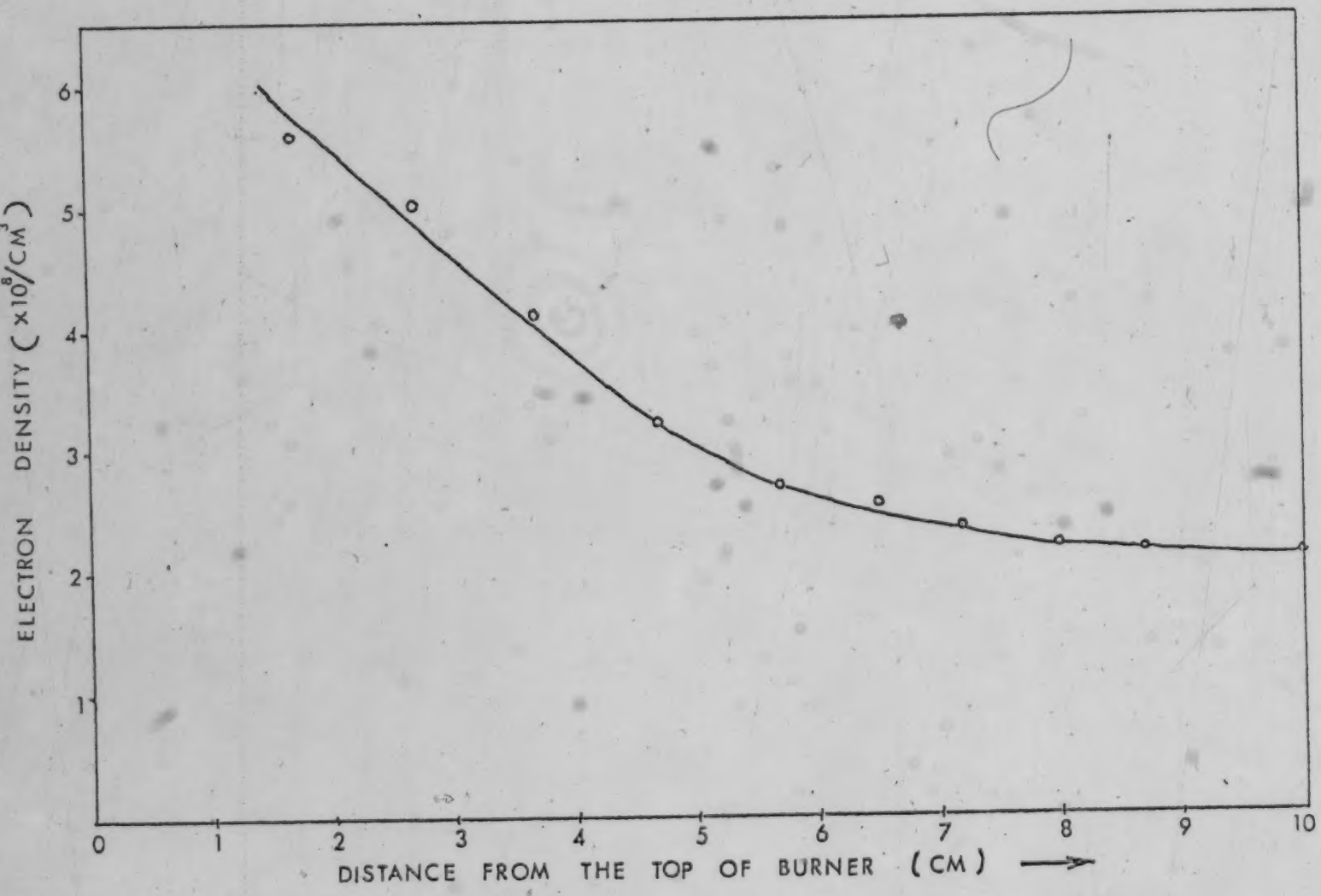

FIGURE (6) Fall off of ionization density with distance above the burner top.

ranges by changing the concentration of the solution. The ionization of the metal is not restricted to the reaction zone, but occurs throughout the burnt gases. In the reaction zone, the dominant process of ionization is "chemi ionization". The dominant positive ion H_3O^+ is produced due to chemi ionization, which reacts with the metal atoms in a process shown below[24]

$$A + H_3O^+ \longrightarrow A^+ + H_2O + H$$

Where A = alkali metal

This transferred chemi-ionization is capable of producing values of $[A^+]$ well above those appropriate to thermal equilibrium which persists into the reaction zone. The ionization in the experimental flame was increased by potassium seeding which is being carried out by the seeding apparatus shown in fig. (7). A solution of KOH was placed in three neck flask. Two electrodes carrying a high voltage were placed at the two extreme necks - the cathode being placed deep into the solution and the anode remaining a few mm above the solution. About 15 kV ac was applied at the two electrodes through an auto-transformer and a high voltage step-up transformer. The electrical spark between the anode and KOH solution surface started around 15 kV and once

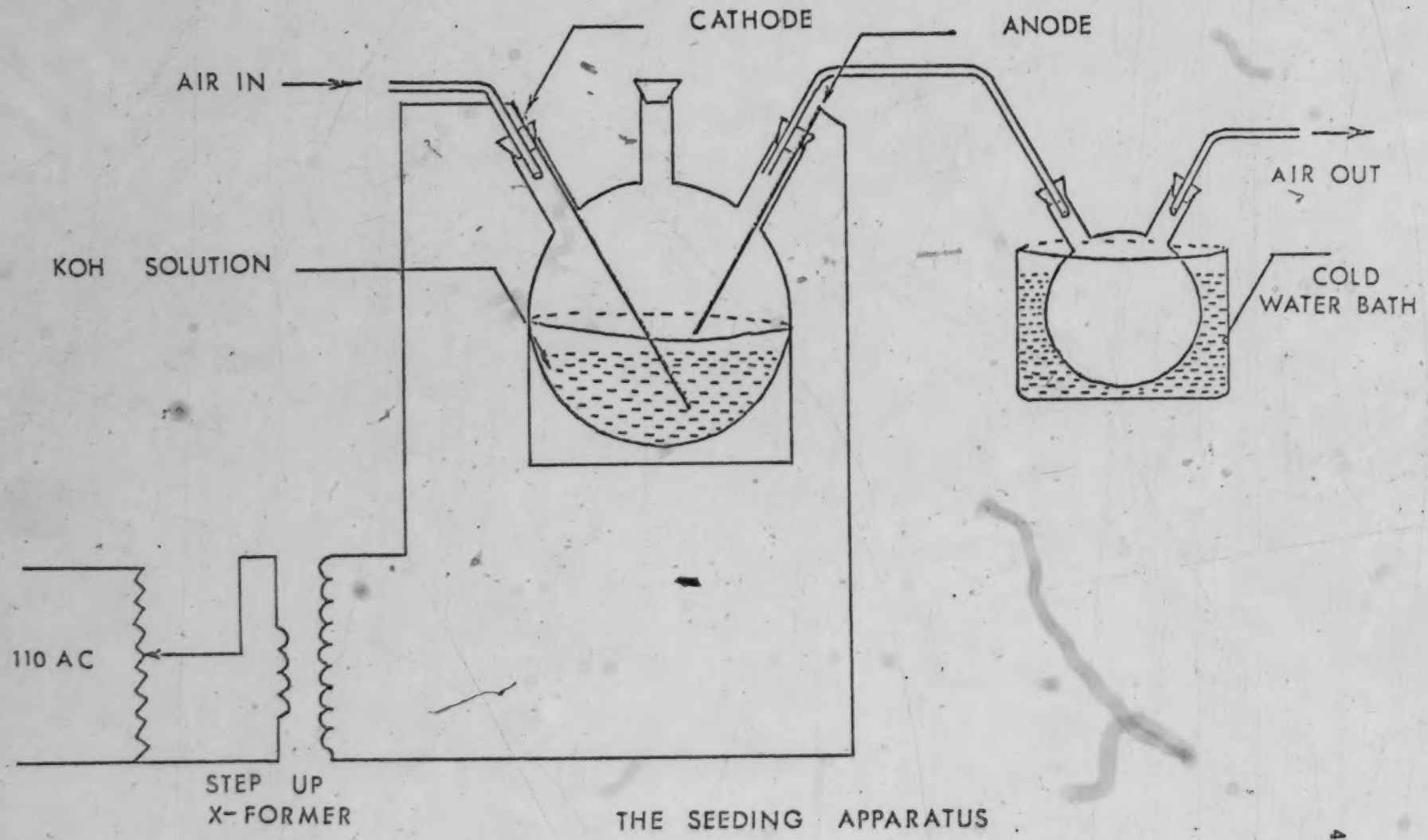

THE SEEDING APPARATUS

FIGURE (7)

the sparking started the voltage could be reduced to about 10 kV just to maintain the spark. The spark atomized the KOH solution and potassium particles were carried away by the flowing air to the burner. Due to the spark, some water vapour was also carried by the outgoing air from the spark chamber to a cooling system. Water vapour condensed in the cooling chamber and dry air with potassium entered the burner. A 1/16" diameter 2% thoriated tungsten rod was used as a cathode and 1/8" diameter 2% thoriated tungsten rod as anode. By changing the concentration of solution, the level of seeding was altered. To change the concentration, the entire solution was changed and a new solution of different concentration poured into the flask.

3.4 STRUCTURE OF THE LANGMUIR PROBE

Throughout the experiment, an air cooled brass probe with an outer diameter of 1/16" and an inner diameter of 1/32" is used. High pressure air was passed through the probe to keep it cold. The air pressure could be regulated from 0 to 15 lb/sq. inch.

3.5 STRUCTURE OF THE GRID

The grid structure shown in fig. (8) is made with small brass tubes of outer diameter 1/16" and inner diameter of 1/32" bent to 90° at both ends and inserted

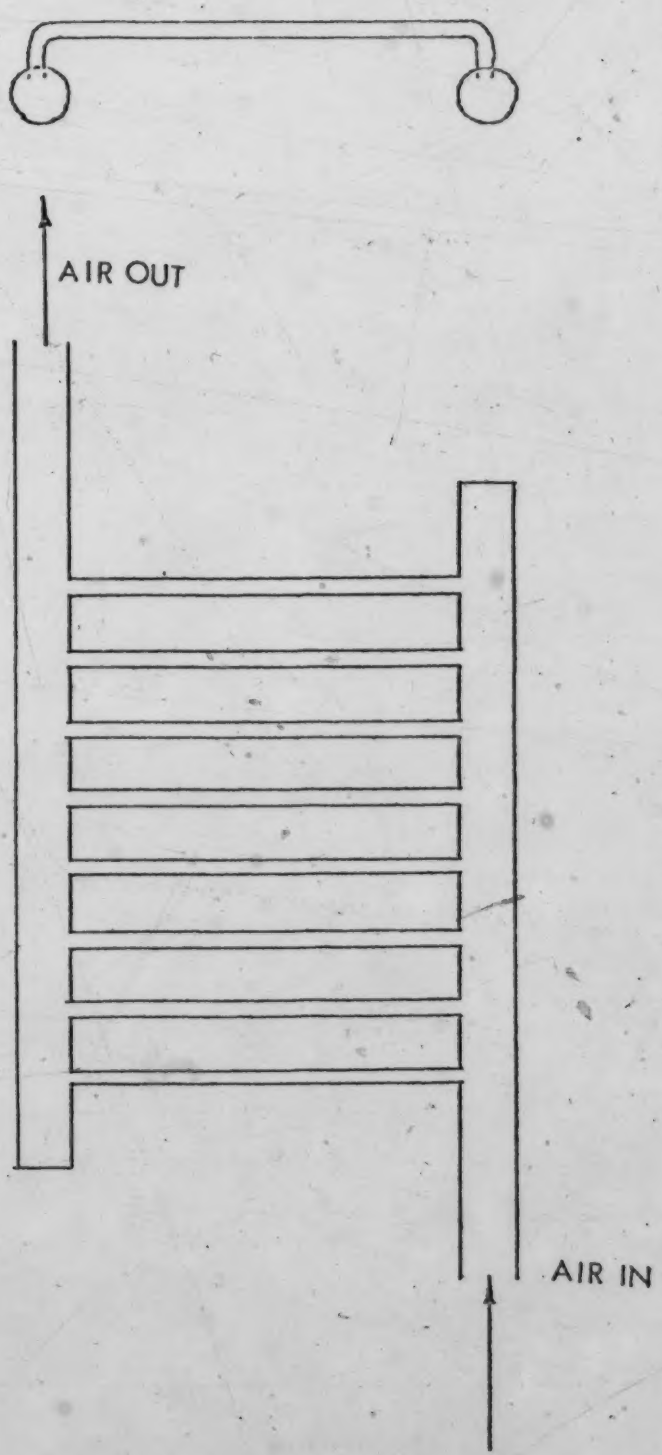

THE STRUCTURE OF GRID

FIGURE (8)

into bigger tubes of 1/4" diameter. Soft solder is applied at the junction points. One of the sides of these bigger tubes is closed and polyflow tubes of 3/8" diameter is connected to the open ends using a 1/4" by 3/8" junctions. High pressure air of about 70 lb/sq. inch flows through the grid to keep it cold.

3.6 ELECTRON DENSITY MEASUREMENT

Two methods are used to measure the electron density of the experimental flame, namely the "saturation grid current" and the "negative probe for ion current". The grid described in Section 3.5 is placed on the flame plasma and is biased negative with respect to the burner with the help of a fluke 412-B high voltage power supply, the polarity of which can be changed with respect to ground. The voltage is varied and the current is measured by a Keithley 153 ammeter until a saturated grid current is obtained. At low grid voltage, the sheath around the probes remains small and the current increases with the increase of voltage. At higher voltage, the sheath formed around the probes of the grid expands to such an extent that the sheath overlap each other. As the voltage is increased further, the sheath does not expand in a horizontal way, but expands like a planar sheath in the vertical direction. The rate at which the ions are formed is equal to the rate

at which they are being attracted by the grid. Consequently, the grid current saturates with the grid voltage.

The grid is moved to different parts of the flame and the electron density is calculated from the saturated grid current using the formula $I = en_e v_f A$ where A = cross section area of flame. An electron density of $2 \times 10^{14}/m^3$ is calculated from the saturated grid current which was placed at a height of 10 cm from the top of the burner. The current-voltage characteristics of the grid from which the electron density is being calculated is shown in fig. (9).

The electron density is also measured by placing a negatively biased probe in the plasma, the electron density being calculated from the equation (4) provided that r_o/r_p is greater than 2.

3.7 MEASUREMENT OF ION DENSITY IN A PLANAR SHEATH

Measurements in a thick planar sheath are accomplished by placing an air cooled grid biased to -400V with respect to a burner about 8 cm above the flame. The electron density at that height of the flame is calculated from the saturation grid current method described in Section (3.6) and is found to be $\sim 2 \times 10^{14}/m^3$. A sheath of about 2 cm thickness is generated below the grid at -400V, at a density of $2 \times 10^{14}/m^3$. The

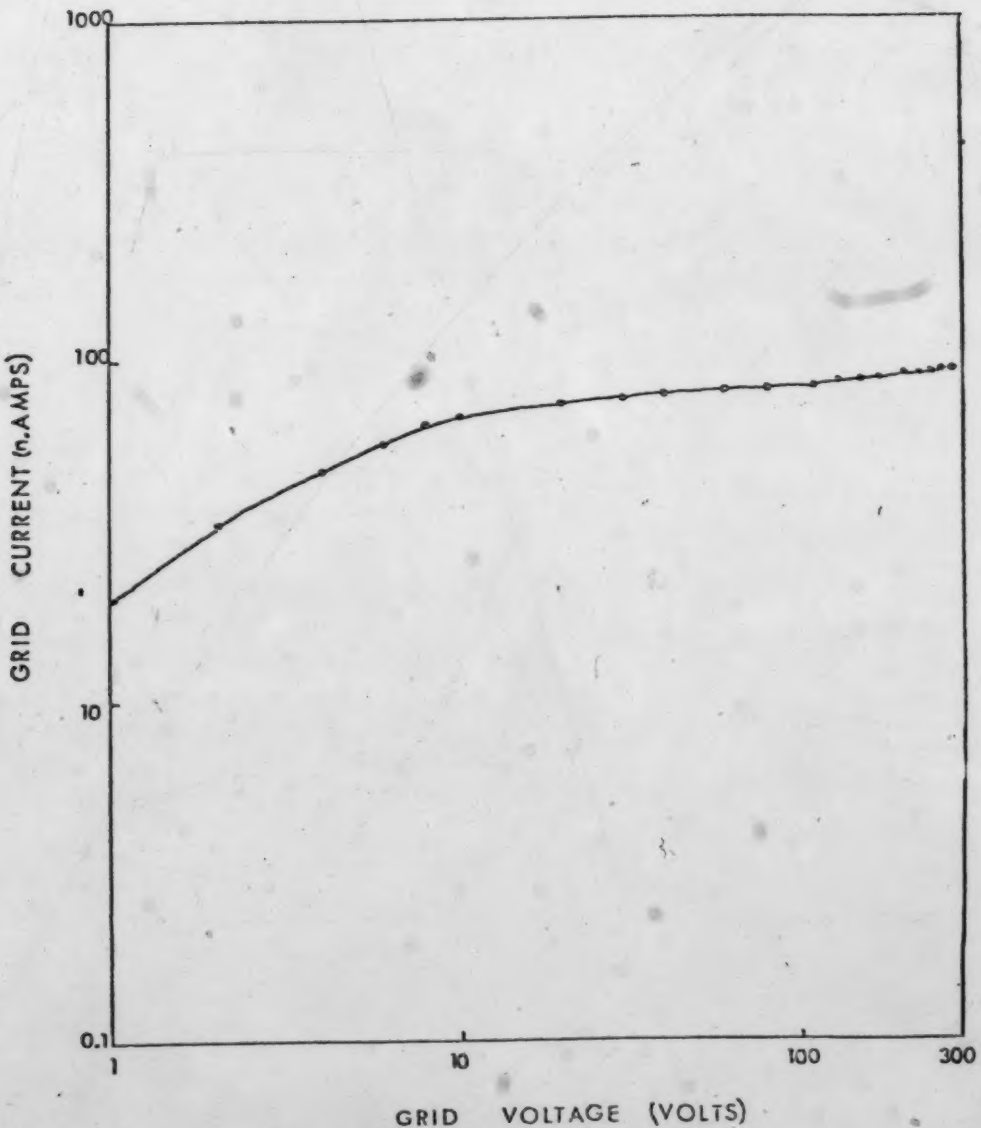

FIGURE (9) The grid current as a function of grid voltage measured at a distance of 10 cms from the top of the burner.

probe is biased positive with respect to the grid with the help of a Fluke power supply and a Keithley 153 microvolt ammeter is used as a null point detector. The probe voltage is then increased until the null point is obtained and then the probe is biased -10V with respect to this space potential. The current collected by the probe at that negative voltage gives the information about the ion density at that particular point in the sheath. The probe is then moved up and down with respect to the grid and the same procedure is repeated. The ion current is measured inside the plasma in the same way. This result is shown in fig. (10). The space potential inside and outside the sheath is measured using the null deflection technique. This is also shown in fig. (11).

3.8 VELOCITY AND TEMPERATURE MEASUREMENT AT THE TOP OF THE CHIMNEY

The temperature at the top of the chimney where the probe was placed is measured a Leeds and Northrup Optical pyrometer, no 8621-C, and then compared to the thermocouple measurement. A copper-constantine thermocouple is used.

The velocity v_f of the gas is calculated from the tracks of illuminated Aluminum oxide which is injected at the bottom of the chimney and then photographed with

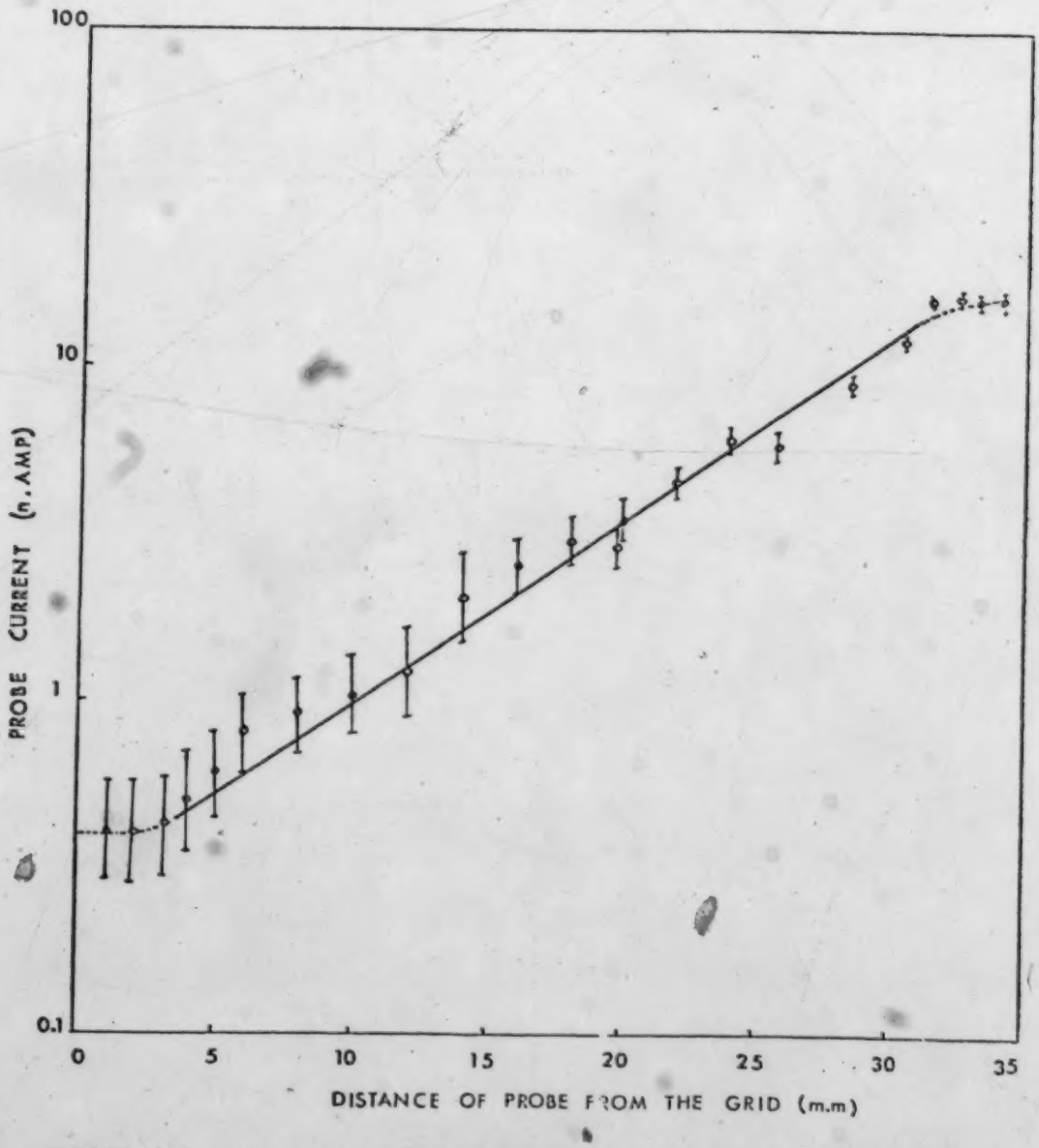

FIGURE (10) The variation of ion current inside and outside the sheath.

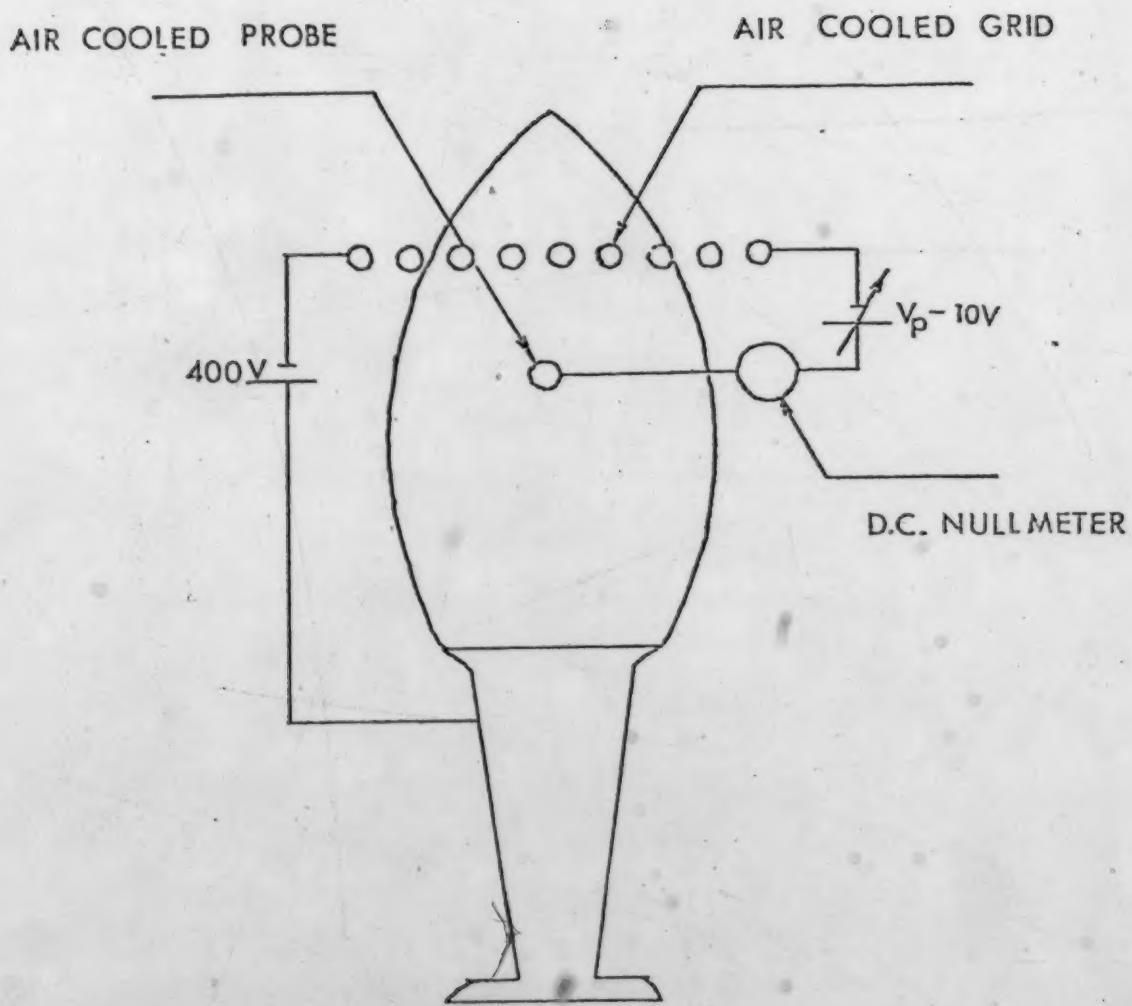

FIGURE (11) The circuit diagram for the measurement of space potential and ionization density in the flame.

a known shutter speed. The shutter speed is measured using a light source, photodiode and oscilloscope. A mean value of the distances travelled during the shutter opening is measured and the velocity v_f is calculated from the known shutter speed. This velocity is found to be equal to 185 cm/sec.

CHAPTER IV

DISCUSSION

The measurements were carried out in a plasma to verify that with the appropriate variation of $\frac{R_e^{\alpha}}{\sqrt{x}}$ the current did indeed change from the sheath/convection current to the field limited current. Measurements were also carried out in a thick planar sheath. The latter measurements had two purposes, the first to check the feasibility of convection measurements in the sheath, the second to utilize a useful property of the sheath - the ability to produce a large change in ion velocity (i.e. in $\mu_i E$) while at the same time keeping the product (ion density x ion velocity) constant. The sheath convection current $I = F(n_o e\ v_f)$ under these conditions would remain constant while the field limited current would vary with the ion density.

The ion density at different portions of the flame was determined from the relationship $n_o = \frac{i}{ev_f A}$ where A = cross-sectional area of the flame, i = the total saturated grid current. The ionization density was observed to remain fairly constant throughout the flame except in the combustion region of the flame. By working at different distances from the burner top, it was possible to sample a range of ionization density of from $2 \times 10^{14}/m^3$ (at $\sim$10 cm from the top of the burner) to $\sim 2 \times 10^{12}/m^3$ (at $\sim$30 cm from the burner at the top

of the glass chimney).

Current-voltage characteristics shown in fig. (12 a,b) were measured at lower densities with the probe situated above a glass 'chimney' which confined the hot gases. The characteristics were calculated from equation (24) by putting the value of the plasma density 'n_o' calculated from the saturation grid current when the density is $2 \times 10^{14}/m^3$ and from the ion probe current using equation (5) when the density is $2 \times 10^{12}/m^3$. The theoretical and experimental current showed fairly good agreement at the two densities $2 \times 10^{14}/m^3$ and $2 \times 10^{12}/m^3$ whereas the thick sheath theory of Clements and Smy[21] and the well known static continuum theory of Su and Lam[5] show very large errors.

In the case of probe potentials ranging from 1 to 10V the experimental points did not follow the theoretical curve because in this low probe potential region the value of log (r_o/r_p) remained less than 1.

To verify the theory of probe measurement in a thick sheath condition, a planar sheath of about 2 cm was generated below the grid at a density of $2 \times 10^{14}/m^3$. By considering the flux of ions up the flame to be constant $n_e(\mu_i E + v_f) = n_o v_f$, it is possible to calculate the electron density n_e at any point in the sheath from the measured E-field at that point. The E-field was

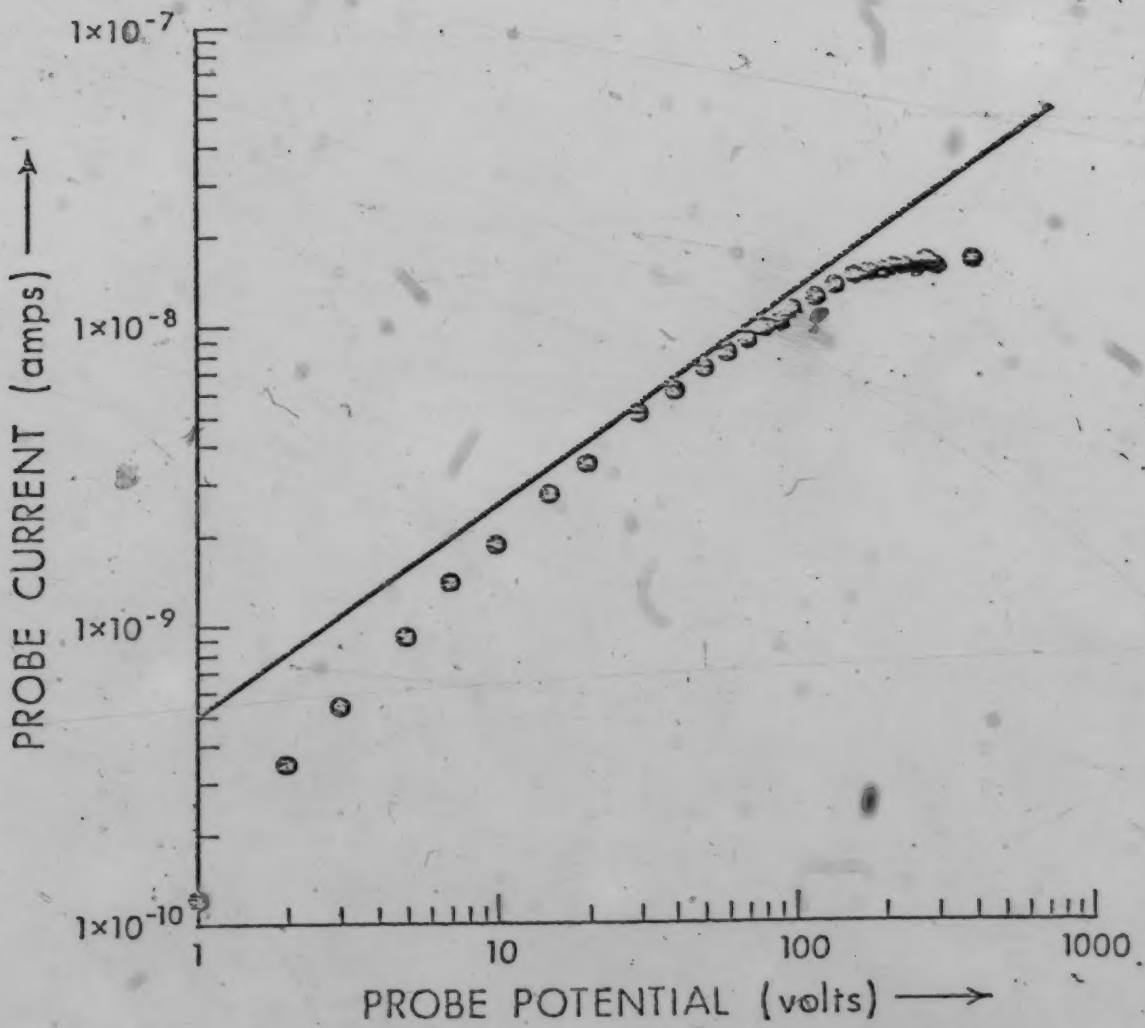

FIGURE (12-a) The current voltage characteristics of a cylindrical probe. The solid line shows the theoretical probe current according to equation (24) and the circles are the experimental probe current at density $n_o = 1.7 \times 10^{12}/m^3$.

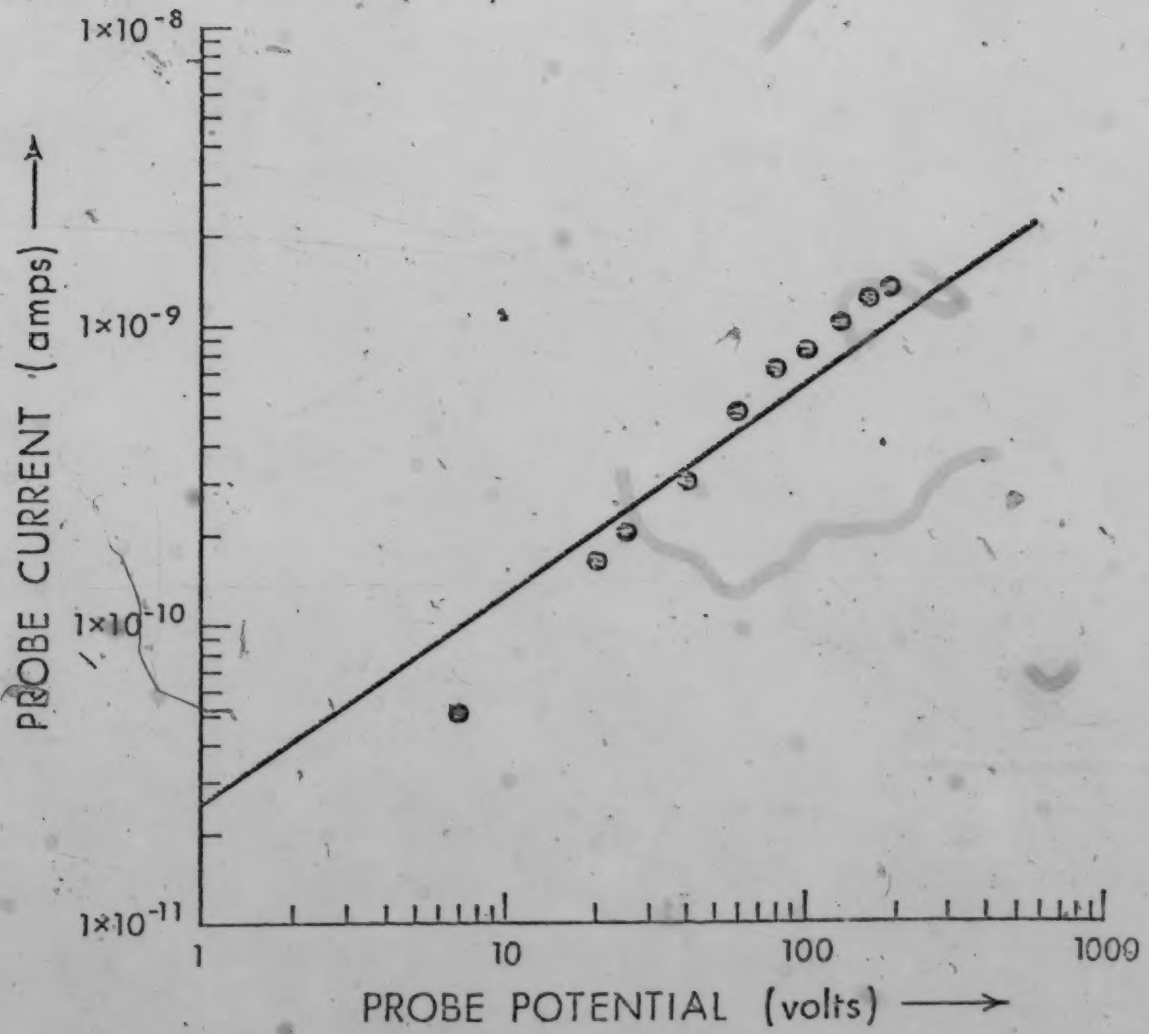

FIGURE (12-b) The current voltage characteristics of a cylindrical probe. The solid line shows the theoretical probe current according to equation (24) and the circles are the experimental probe current at density $n_o = 1.7 \times 10^{13}/m^3$.

calculated by determining the space potential of the plasma, at every point inside and outside the sheath. The spacial determination of the space potential at the sheath edge was very difficult, because the sheath edge vibrated slowly. Consequently, at every instant the potential changed. Again, the determined space potential was not very accurate because the ± 5n.A. scale was used for the null current technique. It was found that the E-field follows the well known space charge equation which decreases away from the grid. From figs. (10)and(13)the measured ion current inside the sheath was observed to be inversely proportional to the electric field. The ion current also increases at a constant rate through the sheath but saturates close to the grid and sheath edge. The reasons for this saturation is not clearly understood.

The measurements of fig. (14) show some of the earlier measurements of Clements and Smy[21] and together with some of those of fig. (12 a,b). All currents are normalized with respect to the calculated sheath/ convection current. These normalized currents are shown as a function of the parameter $\frac{Re_a}{\sqrt{x}}$. The theoretically calculated sheath/convection currents are shown as a horizontal line and the field limited current by

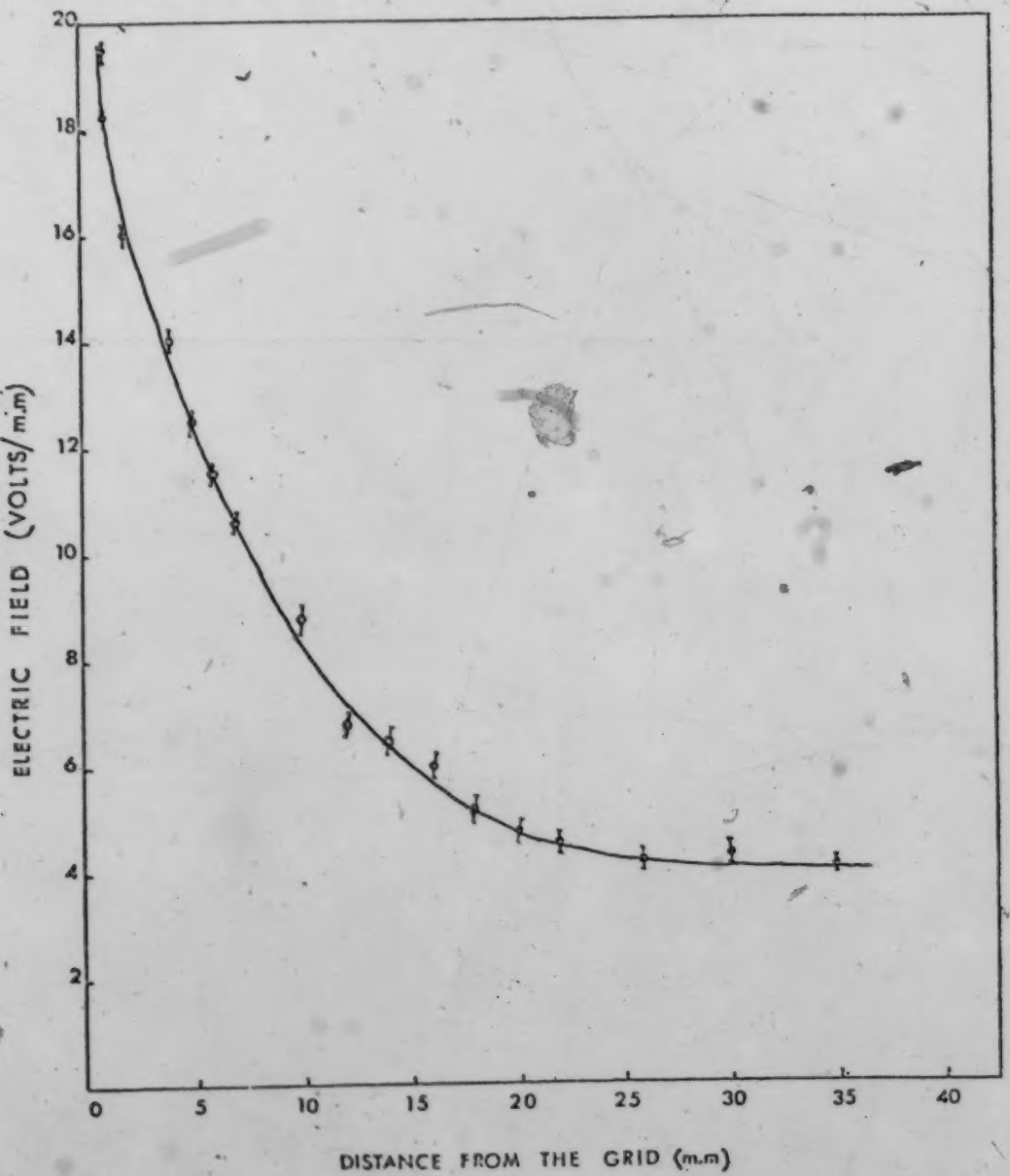

FIGURE (13) The variation of electric field inside and outside the sheath.

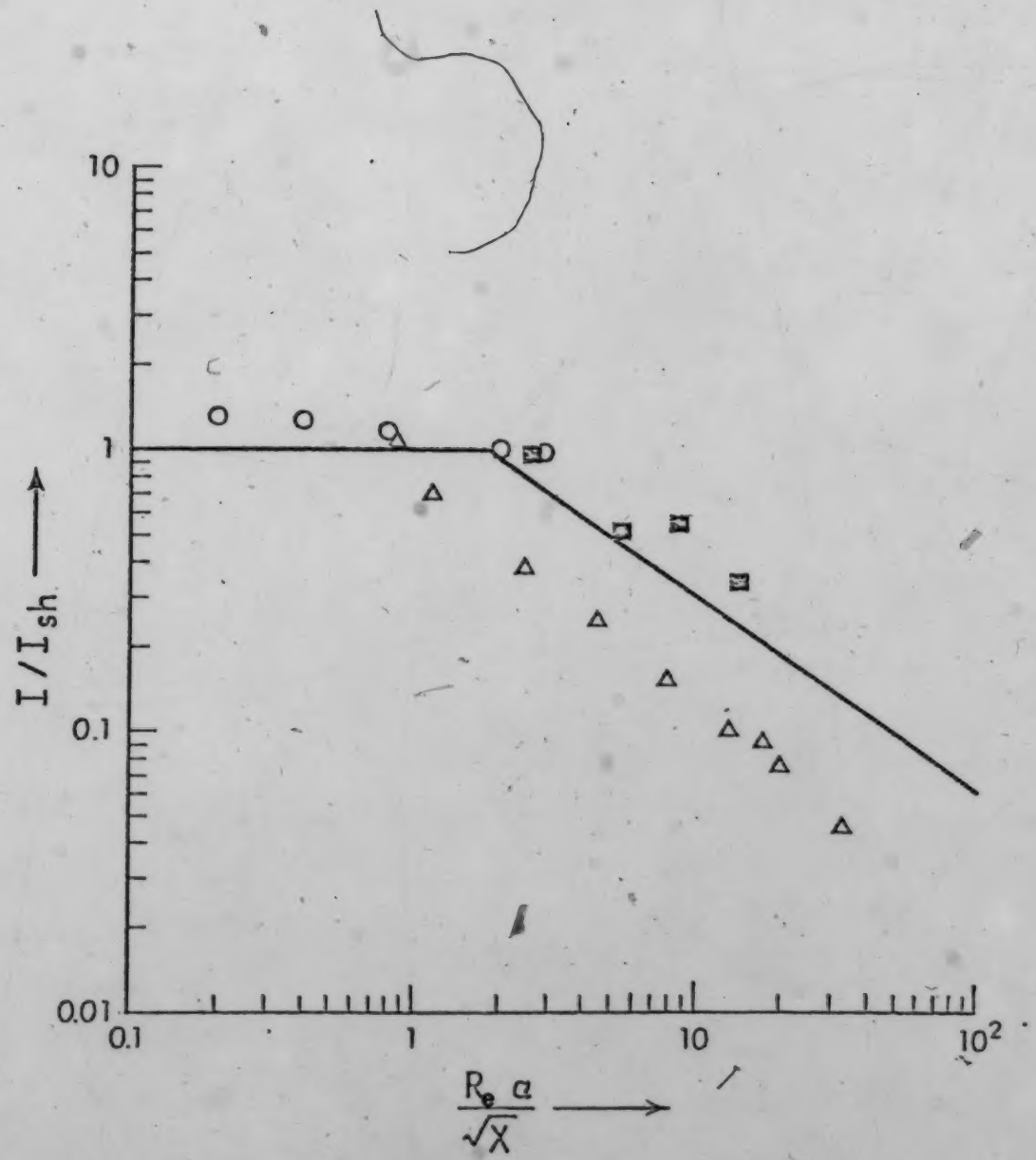

FIGURE (14) The transition from sheath/convection to field limited current of a cylindrical probe shown with the variation of $\frac{R_e a}{\sqrt{X}}$

- ● Clements and Smy from ref-21
- ■ In plasma at the top of the chimney
- ▲ Inside the sheath

The horizontal solid line is calculated from the sheath/convection theory and the solid sloping line is from field limited current theory.

the sloping line. At higher densities, $4 \times 10^{15}/m^3$ to $2 \times 10^{18}/m^3$, Clements and Smy observed that the probe follows the sheath/convection current theory and their experimental points are shown by circles in fig. (14), which shows good agreement in the range of $\frac{R_e \alpha}{\sqrt{x}} \leq 1$. When $\frac{R_e \alpha}{\sqrt{x}}$ exceeds 1, the probe current does not follow the sheath/convection theory. At low ionization, $\frac{R_e \alpha}{\sqrt{x}}$ becomes much greater than unity and the ions entering into the sheath do not reach the probe because of the weak E-field present in the sheath. The field limited theory shows good agreement with the experiments; those performed at low densities are indicated by the squares, and those measured inside the sheath are indicated by the triangles.

The ion mobility used in these calculations is taken from the most recent value for chemi-ionization given by Bradley and Ibharim [30] of 8×10^{-4} $m^2/V\text{-sec}$ at atmospheric pressure and 2000° K. The mobility is scaled with temperature from the measurements performed at low temperature. The average flow velocity of the plasma is calculated from the statistical mean of the particle trace length on the photographic plate exposed at a known shutter speed.

The technique of measuring the variation of ion current with probe bias to determine the ion density

would seem to be a useful one.

From the point of view of ionization measurements the experimentalist has enough variables at hand to avoid the region $\log (r_o/r_p) \leq 1$ (namely bias voltage, probe radius, probe/plasma velocity) for all but high ion densities or large diameter water cooled electrodes.

CHAPTER V

Conclusions

From the results shown in figs. (14) it is clear that for $\frac{R_{ea}}{\sqrt{x}} > 1$, the sheath/convection formula is erroneous whereas the field limited current agrees reasonably well with the experiment. The sheath measurements not only show agreement with theory but also provide convincing proof that the space charge limited current model $I = 1(n_o v_f)$ is not applicable for $\frac{R_{ea}}{\sqrt{x}}$ since the slope of the plots would be zero in this case. Together with the earlier results of Clements and Smy[21] the measurements show that it is always the lesser of the sheath/convection and field limited currents which is appropriate.

These measurements, of course, do not constitute a comprehensive test of the field limited current model. In particular, no measurements have been carried out with large probe or spherical probe geometries. However, the experimental results given here do provide strong evidence for the basic principles of the theory.

It is interesting to consider some implications of these theoretical and experimental results. First, it is evident that at low plasma velocities, the sheath convection model is adequate down to densities of $\sim 10^{13}/m^3$. Since there exists substantial theoretical and experimental evidence to show that the model can

work at densities as high as $\sim 10^{22}/m^3$ (Clements, Kerr, Offenberger and Smy)[31] we see that the sheath/convection model in itself is in fact of broad application. At higher velocities, the $\frac{R_e a}{\sqrt{x}} < 1$ limitation becomes more dominant. For instance, in shock tube or plasma jet studies near atmospheric pressure, velocities $\sim 10^3$ m/sec or more are common. With flame velocities ~ 1 m/sec we see that the increase in R_e will be a factor of $\sim 10^3$ necessitating an increase in n_o ($\alpha \frac{1}{\sqrt{a}}$) of 10^6 (i.e. to $10^{20}/m^3$). Thus it can be expected that the field limited current model be of considerable application at high velocities. It is important to note here that the parameter $R_e a$ is not affected by the probe dimensions and thus we cannot move into a preferred regime of operation by merely changing the probe dimensions.

The equations for cylindrical and spherical probes in a moving plasma for the situation where the probe current is field limited, are deduced. No comprehensive experimental check of these equations has been made. However, it has been established that with increasing $\frac{R_e a}{\sqrt{x}}$, the transition to field limited current does occur at the right point and the current is of the expected magnitude.

SUGGESTIONS FOR FUTURE WORK

The recombination co-efficient of the plasma seeded with any other alkali material can be calculated using these probe theories to measure the electron or ion densities with respect to time after collapsing a planar sheath produced in the described way. Again the transition from the sheath to the plasma can be calculated using the same probe theory at least in the case of weakly ionized plasma. The transit time of ions can be determined by vibrating this type of planar sheath, superimposing an ac voltage on a dc voltage.

REFERENCES

1. Jensen, D.E. and Travers, B.E.L., IEEE Trans Plasma Science, 34 (1974).

2. Soundy, R.G. and Williams, H., AGARD Spec. Publication No. 8,161 (1965).

3. Langmuir, I., in "Collected Works of Irving Langmuir (G. Suits ed.) Vol.4, MacMillan (Pergamon) New York (1961).

4. Schuiz, G.J. and Brown, S.C., Phys. Rev., Vol. 98 1642 (1955).

5. Su, C.H. and Lam, S.H., Phys. Fluids, Vol. 6, 1479 (1963).

6. Lam, S.H., AIAAJ, Vol. 2, 256 (1964).

7. Talbot, L., Phys. Fluids, Vol. 3, 289 (1960).

8. Turcotte, D.L. and Gillespie, J., AIAAJ Vol. 1, 2293 (1963).

9. Chung, P.M. Phys. Fluids, Vol. 7, 110 (1964).

10. Chung, P.M., AIAAJ, Vol 3, 817 (1965).

11. Chung, P.M. and Blankenship, V.D., AIAAJ, Vol. 4, 442 (1966).

12. Su, C.H., AIAAJ, Vol. 3, 842 (1965).

13. De Boer, P.C.T. and Johnson, R.A., Phys. Fluids, Vol. 11, 909 (1968).

14. De Boer, P.C.T., AIAAJ, Vol. 11, 1012 (1973).

15. Clements, R.M. and Smy, P.R., J. Appl. Phys., Vol. 41, 3745 (1970).

16. Clements, R.M. and Smy, P.R., J. Phys. D., Vol. 6, 184 (1973).

17. Kulgein, N.G., AIAAJ, Vol. 6, 151 (1968).

18. Clements, R.M. and Smy, P.R., Proc. IEE, Vol. 117, 1721 (1970).

19. Hoult, D.P., J. Geophys. Res, Vol. 70, 3183 (1965).

20. Sonin, A.A., J. Geophys. Res., Vol. 72, 4547 (1967).

21. Clements, R.M. and Smy, P.R., J. Appl. Phys., Vol. 40, 4553 (1969).

22. Lawton, J. and Weinberg, F.J., 'Electrical Aspects of Combustion', Clarendon Press, Oxford (1969).

23. Fristrom, R.M. and Westenberg, A.A., 'Flame Structure', McGraw Hill, (New York, U.S.A.) (1965).

24. Sugden, T.M., '10th. International Conference on Phenomena in Ionized gases' (Donald Parsons and Co. Ltd., Oxford England) 437 (1971).

25. Calcote, H.F., 8th. Symposium (International) on Combustion, 184, (1962).

26. Calcote, H.F., 9th. Symposium (International) on Combustion, 622, (1963).

27. Poncelet, J. and Berendsen, R. and Tiggelen, A., 'Seventh Symposium (International) on Combustion, 256 (1961).

28. King, I.R., J. Chem. Phys., Vol. 31, 855 (1960).

29. Gaydon, A.G. and Wolfhard, H.G., 'Flames, their Structure, Radiation and Temperature', Chapman and Hall, London (1953).

30. Bradley, D. and Ibrahim, M.A. Said, J. Phys. D., Vol. 7, 1377 (1974).

31. Clements, R.M., Kerr, R.D., Offenberger, A.A. and Smy, P.R., Electronics Letters, Vol. 8, 361 (1972).